FREQUENCY INVARIANT BEAMFORMING AND ITS APPLICATION TO WIDEBAND DIRECTION OF ARRIVAL ESTIMATION

A THESIS SUBMITTED TO
THE GRADUATE SCHOOL OF NATURAL AND APPLIED SCIENCES
OF
MIDDLE EAST TECHNICAL UNIVERSITY

BY

EREN BABATAŞ

IN PARTIAL FULLFILLMENT OF THE REQUIREMENTS
FOR
THE DEGREE OF MASTER OF SCIENCE
IN
ELECTRICAL AND ELECTRONICS ENGINEERING

SEPTEMBER 2008

Approval of the thesis:

FREQUENCY INVARIANT BEAMFORMING AND ITS APPLICATION TO WIDEBAND DIRECTION OF ARRIVAL ESTIMATION

submitted by Eren Babataş in partial fulfillment of the requirements for the degree of Master of Science in Electrical and electronics Engineering Department, Middle East Technical University by,

Prof. Dr. Canan Özgen _____
Dean, Graduate School of Natural and Applied Sciences

Prof. Dr. İsmet Erkmen _____
Head of Department, Electrical and Electronics Engineering Dept.

Assist. Prof. Dr. Çağatay Candan _____
Supervisor, Electrical and Electronics Engineering Dept.

Examining Committee Members:

Prof. Dr. Engin Tuncer _____
Electrical and Electronics Engineering Dept., METU

Assoc. Prof. Dr. Sencer Koç _____
Electrical and Electronics Engineering Dept., METU

Assist. Prof. Dr. Çağatay Candan _____
Electrical and Electronics Engineering Dept., METU

Assist. Prof. Dr. Behzat Şahin _____
Electrical and Electronics Engineering Dept., METU

Aydın Bayri (MSc.) _____
ASELSAN

Date : September 23, 2008

I hereby declare that all information in this document has been obtained and presented in accordance with academic rules and ethical conduct. I also declare that, as required by these rules and conduct, I have fully cited and referenced all material and results that are not original to this work.

Name, Last name : Eren Babataş

Signature :

ABSTRACT

FREQUENCY INVARIANT BEAMFORMING AND ITS APPLICATION TO WIDEBAND DIRECTION OF ARRIVAL ESTIMATION

Babataş, Eren

M. Sc., Department of Electrical and Electronics Engineering

Supervisor: Assist. Prof. Dr. Çağatay Candan

In this thesis the direction of arrival estimation of wideband signals using frequency invariant beamforming method is examined. The difficulty with the direction of arrival estimation of wideband signals is that it is not possible to obtain a single covariance matrix valid for the whole frequency spectrum of the signal. There are various methods proposed in the literature to overcome this difficulty. The common aim of all the methods is to obtain a composite covariance matrix for the overall band of the signal.

In this thesis, we concentrate on a method in [12]. This method is based on a beamforming technique that provides frequency invariant beams in the band of interest. Therefore there is no need for frequency decomposition as it is done with the other wideband methods. A comparison of the frequency invariant beamforming method with coherent signal subspace methods and narrow band methods is also given.

Keywords: Direction of arrival estimation, frequency invariant beamforming.

September 2008, 85 pages

ÖZ

FREKANS DEĞİŞMEZ HUZMELEME VE BU YÖNTEMİN GENİŞBANT YÖN BULMAYA UYGULANMASI

Babataş, Eren

Yüksek Lisans, Elektrik Elektronik Mühendisliği Bölümü
Tez Yöneticisi: Yrd. Doç. Dr. Çağatay Candan

Bu tezde genişbant sinyallerin geliş açılarının frekans değişmez huzmelemeye dayanan bir yöntem kullanılarak kestirilmesi üzerinde çalışılmıştır. Genişbant sinyaller ile alt uzay tabanlı yöntemleri kullanırken karşılaşılan ana problem sinyalin tüm frekans bandı için tek bir kovaryans matrisinin elde edilememesidir. Literatürde bu problemi çözmek için çeşitli yöntemler bulunmaktadır, bu yöntemlerin ortak amacı ise tüm banttaki bilgiyi içeren tek bir kovaryans matrisi elde etmektir.

Bu tezde esas olarak referans [12] de verilen bir yöntem üzerinde durulmaktadır. Bu yöntem ilgilenilen frekans bandında frekans değişmez örüntüler elde edilmesini sağlar. Böylece, diğer yöntemlerde yapıldığı gibi, frekans bandını parçalara ayırıp işlemek durumunda kalmayız. İlgilenilen yöntem ayrıntılı bir şekilde ele alındığı gibi, başka bir genişbant yöntem ve bazı darbant yöntemlerle de karşılaştırılmıştır.

Anahtar Kelimeler: Varış yönü kestirimi, frekans değişmez huzmeleme

Eylül 2008, 85 sayfa

ACKNOWLEDGEMENTS

I would like to express my deepest gratitude to my supervisor Assist. Prof. Dr. Çağatay Candan for his encouragements, guidance, advice, criticism and insight throughout the research. I would also like to thank Dr. Engin Tuncer, Dr. Sencer Koç, Dr. Behzat Şahin and Aydın Bayri for their comments and contributions.

I would like to thank ASELSAN Inc. for facilities provided for the competition of this thesis.

TABLE OF CONTENTS

LIST OF FIGURES

LIST OF ABBREVIATIONS

DOA: Direction Of Arrival

RMS: Root Mean Square

SNR: Signal to Noise Ratio

MUSIC: Multiple Signal Classification

CSSM: Coherent Signal Subspace Method

FIB: Frequency Invariant Beamforming

CHAPTER 1

INTRODUCTION

1.1 Background

Direction of arrival (DOA) estimation of an incoming wave is a classical problem occurring in wireless communications, radar signal processing, acoustic signal processing. Subspace methods, which are also called high resolution methods, are widely used when it is required to estimate the DOA of one target with high accuracy or the DOA' s of multiple targets. The subspace methods are based on the estimation of the covariance matrix of signal snapshots. The DOA information is retrieved using the eigenspace decomposition of the covariance matrix. Methods such as Pisarenko, MUSIC, Min-Norm, ESPRIT are some of well known subspace methods.

In this thesis we examine the DOA problem for wideband signals. Some signals of interest have wideband spectrum due to their application requirements such as low probability of interception (LPI) operation or high radar range resolution. The classical subspace solutions are based on some narrowband assumptions. Therefore, as said in literature, these methods can't be directly used when the signal of interest is wideband.

In this thesis, our goal is to examine the wideband DOA estimation method based on frequency invariant beamforming, compare it with other wideband methods and compare it with its narrowband counterparts.

1.2 Outline

In this study DOA estimation of wideband signal sources by frequency invariant beamforming method is considered. Wideband DOA methods examined can be classified into four categories: Incoherent methods, coherent methods, method based on array interpolation and method based on frequency invariant beamforming (FIB).

The incoherent method processes each frequency bin independently and average the DOA estimates over all the bins. Since each frequency bin is processed independently from others, we can use any narrowband method to estimate DOA for each bin. This method can be considered as the application of narrowband DOA methods to multiple frequencies and fusing the DOA estimates generated by each frequency bin with simple averaging operation.

One of the most well known wideband DOA estimation methods is Coherent Signal Subspace Method (CSSM), which is a member of coherent methods. With this method, the incoming signal is first decomposed into frequency bands and each band is transformed into a reference band through a focusing matrix. The method requires an initial DOA estimation and its performance depends on the focusing matrix. In this thesis, the CSSM method is implemented and its performance is compared with the methods based on FIB. The other coherent methods are Beamforming Invariance Coherent Signal Subspace Method (BICSSM), and Weighted Average of Signal Subspaces for robust wideband direction finding (WAVES). These methods are briefly explained in Chapter 3.

Array interpolation is an alternative technique for DOA estimation of wideband signal sources. It uses virtual arrays with the same manifold for different frequency bins to obtain a composite covariance matrix.

The main method that is examined in this thesis is the frequency invariant beamforming (FIB) method. Frequency invariant beamforming method does not

require the incoming signal to be decomposed into narrow frequency bins. The composite covariance matrix is constructed directly from the wideband signal.

The organization of the thesis is as follows: In Chapter 2, we introduce basic assumptions for the DOA estimation of narrowband signals and review some narrowband subspace methods. In Chapter 3, the differences between wideband and narrowband signals will be examined and wideband DOA estimation methods except the one based on FIB method will be introduced. In Chapter 4, FIB methods are explained in detail, and their performances for obtaining frequency invariant beam are evaluated. In chapter 5, the DOA estimation based on Ward& Kennedy's FIB method is explained, its performance is evaluated. Then some performance comparisons between Ward & Kennedy's FIB method and CSSM, between Ward & Kennedy's FIB method and the incoherent method, and lastly between Ward & Kennedy's FIB method and narrowband MUSIC are evaluated.

1.3 PROBLEM STATEMENT

DOA estimation method based on FIB method uses beam shaping filters named as primary filters to obtain a composite covariance matrix for overall frequency band. Since subspace methods like MUSIC need more than one output to obtain the covariance matrix of signals, two or more primary filter banks, i.e., beamformers must be used in the FIB method. If we assume there is only one target, two different beamformers should be enough.

Let's assume that we have 7-element antenna array. For other wideband DOA estimation methods like CSSM, we need a 7-channel receiver to receive signals, amplify them, convert them from analog to digital etc. The calibration of RF components in the processing chain of each receiver imposes significant engineering difficulties and costly to implement. However, if we design analog beam shaping filters and transform 7 dimensional input to a single frequency invariant output, we only a single RF chain per each beamshaping filter bank. The number of channels will be equal to the number of different beamformers. Because of practical restrictions such as cost and channel claibration, decreasing the number of channels will be an advantage for the implementation of the FIB method. In figures below, a 7-element antenna array is given for both CSSM and FIB structures in order.

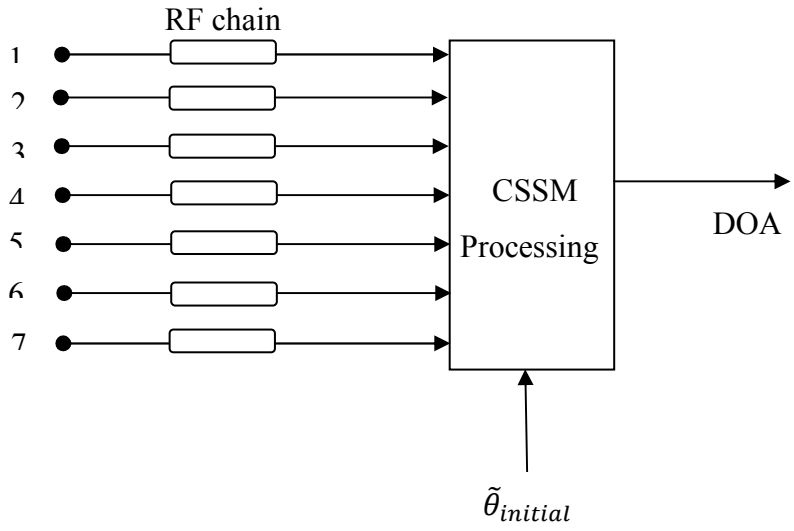

Figure 1.1: CSSM structure for a 7-element antenna array

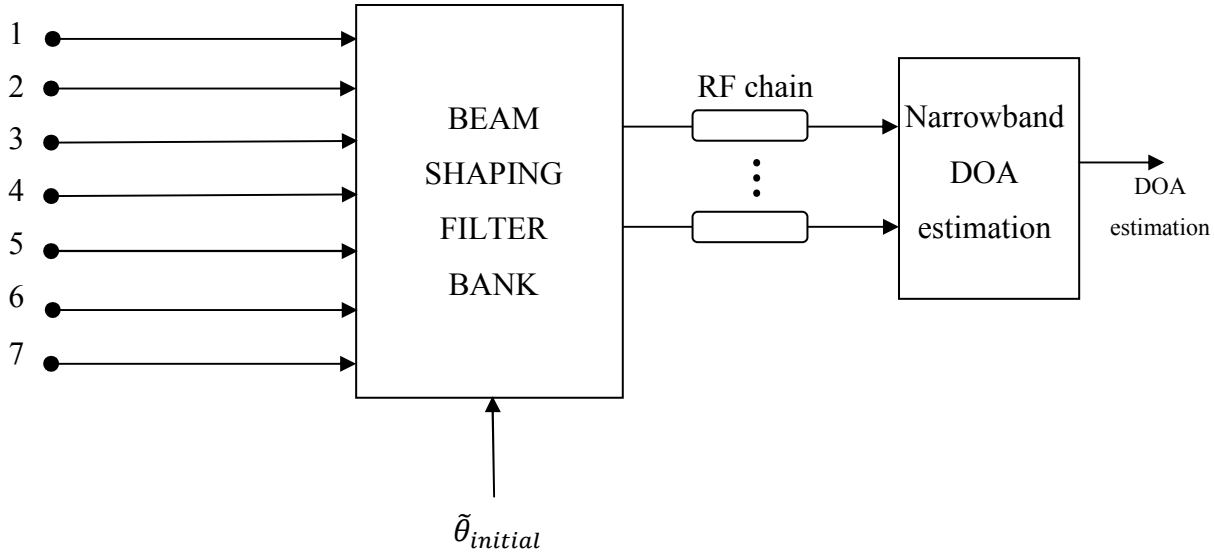

Figure 1.2: FIB structure for a 7-element antenna array

The FIB method doesn't use sensor outputs directly, filters them to obtain overall frequency invariant beams. As a result it doesn't need frequency decomposition, but filtering causes some processing loss. On the other hand, CSSM directly uses sensor outputs to estimate the covariance matrix for each narrow frequency bin and transforms them into a reference bin. Therefore, processing gain will be N times more than processing only one narrow frequency bin where N is the number of narrow frequency bins.

CSSM can show a good performance when the initial estimation error is low, because the design of the focusing matrix is strongly dependent on the initial estimation error. However, the FIB method can be preferrable when there is a relatively high initial estimation error. With the FIB method the iinitial estimation error can be compensated by increasing the FOV (Field Of View) width and number of overall beams formed by beam shaping filters.

In this thesis, we investigate the performance of the FIB method at different levels of initial estimation error and compare its performance with CSSM given in [3] and incoherent method. As discussed above the implementation of FIB is preferable due to its lower cost, when the performance of the FIB method is similar to the others.

CHAPTER 2

INTRODUCTION TO NARROWBAND METHODS

In this chapter, the basic assumptions for narrowband operation is reviewed and some subspace methods are introduced briefly. The presentation mainly follows the reference [1].

2.1 Basic Assumptions for Narrowband DOA Estimation

In narrowband subspace methods, there are two basic assumptions to obtain a simplified signal model. These assumptions are

i) Far-field assumption

ii) Bandwidth assumption

The first assumption states that the incoming waveform of the source signal can be considered as a plane wave upon its arrival.

The second assumption states that the source signal amplitude is constant in the narrowband around the center frequency so that little time delays can be written as phase shift in the time domain. Let us get the narrowband signal as

$$s(t) = \gamma(t).e^{j2\pi f_c t} \tag{2.1}$$

If the signal is delayed by time delay τ, the delayed signal will be

$$s(t-\tau) = \gamma(t-\tau).e^{j2\pi f_c(t-\tau)} \approx \gamma(t).e^{j2\pi f_c t}.e^{-j2\pi f_c \tau} = s(t).e^{-j2\pi f_c \tau} \qquad (2.2)$$

with respect to narrowband assumption.

2.2 Narrowband Subspace Methods

There are many methods in the literature that use subspace structure of the observation vectors [1]. Here we briefly examine some of these methods for the sake of completeness.

We assume there are n signal sources and an m-element antenna array is used to estimate the DOA of the sources. The antennas are assumed to be omni-directional.

2.2.1 MUSIC (Multiple Signal Classification)

MUSIC is derived from the covariance matrix model

$$\boldsymbol{R} \triangleq E\{\tilde{y}(t)\tilde{y}^*(t)\} = \boldsymbol{APA}^* + \sigma^2\boldsymbol{I} \quad ; \qquad \boldsymbol{P} = \begin{bmatrix} \alpha_1^2 & \cdots & 0 \\ \vdots & \ddots & \vdots \\ 0 & \cdots & \alpha_n^2 \end{bmatrix} \qquad (2.3)$$

where

$$\boldsymbol{A} = [\boldsymbol{a}(\theta_1), \ldots, \boldsymbol{a}(\theta_n)] \quad (mxn) \qquad (2.4)$$

$$\boldsymbol{a}(\theta, f) \triangleq \left[1 \; e^{-j2\pi f \frac{d}{c}\sin(\theta)} \; \ldots \; e^{-j2\pi f \frac{(m-1).d}{c}\sin(\theta)}\right]^T \quad (mx1) \qquad (2.5)$$

d: sensor spacing , *c*: the speed of light

$$\tilde{\boldsymbol{y}}(t) \triangleq \begin{bmatrix} y(t) \\ y(t-1) \\ \vdots \\ y(t-m+1) \end{bmatrix} = \boldsymbol{A}\tilde{\boldsymbol{x}}(t) + \tilde{\boldsymbol{n}}(t) \qquad (2.6)$$

$$\tilde{\boldsymbol{x}}(t) = [x_1(t) \quad \dots \quad x_n(t)]^T \tag{2.7}$$

$$\tilde{\boldsymbol{n}}(t) = [n(t) \quad \dots \quad n(t-m+1)]^T \tag{2.8}$$

where $\tilde{\boldsymbol{y}}(t)$ is the vector of channel outputs, $\tilde{\boldsymbol{x}}(t)$ is the vector of the signals received by the antennas and $\tilde{\boldsymbol{n}}(t)$ is the vector of noise. The noise in the channels is assumed to be white noise. The matrix $\boldsymbol{A}$ is the manifold matrix of the sensor array which is a Vandermonde matrix (for uniformly spaced sensors) with the following rank property:

$$\text{rank}(\boldsymbol{A}) = n \text{ if } m \geq n \tag{2.9}$$

DOA estimation is done by the eigen decomposition of the covariance matrix $\boldsymbol{R}$, and the covariance matrix can be found by the dot multiplication of $\tilde{\boldsymbol{y}}(t)$. In MUSIC, it is assumed that $m>n$. Let $\lambda_1 \geq \lambda_2 \geq \cdots \geq \lambda_m$ denote the eigenvalues of the covariance matrix $\boldsymbol{R}$, and let $\{\boldsymbol{s}_1, \ \dots, \ \boldsymbol{s}_n\}$ be the orthonormal eigenvectors associated with $\{\lambda_1, \ \dots, \ \lambda_n\}$, and $\{\boldsymbol{g}_1, \ \cdots, \ \boldsymbol{g}_{m-n}\}$ the orthonormal eigenvectors associated with $\{\lambda_{n+1}, \ \dots, \ \lambda_m\}$.

Since $\boldsymbol{APA}^*$ has n positive eigenvalues, the remaining m-n eigenvalues are equal to zero with the fact that

$$\lambda_k = \check{\lambda}_k + \sigma^2 \quad , \quad k = 1, \dots, m \tag{2.10}$$

where $\{\check{\lambda}_k\}_{k=1}^{m}$ are the eigenvalues of $\boldsymbol{APA}^*$**.** Then

$$\begin{cases} \lambda_k > \sigma^2 \ for \ k = 1, \dots, n \\ \lambda_k = \sigma^2 \ for \ k = n+1, \dots, m \end{cases} \tag{2.11}$$

Let

$$\boldsymbol{S} = [\boldsymbol{s}_1, \quad \cdots, \quad \boldsymbol{s_n}] \quad (mxn) \tag{2.12}$$

$$\boldsymbol{G} = [\boldsymbol{g}_1, \quad \cdots, \quad \boldsymbol{g_{m-n}}] \quad (mx(m-n)) \tag{2.13}$$

From (2.3) and (2.11), we get

$$\boldsymbol{RG} = \boldsymbol{G}\begin{bmatrix} \lambda_{n+1} & \cdots & 0 \\ \vdots & \ddots & \vdots \\ 0 & \cdots & \lambda_m \end{bmatrix} = \sigma^2\boldsymbol{G} = \boldsymbol{APA}^*\boldsymbol{G} + \sigma^2\boldsymbol{G} \tag{2.14}$$

(2.14) implies that $\boldsymbol{APA}^*\boldsymbol{G} = 0$, or

$$\boldsymbol{A}^*\boldsymbol{G} = 0 \tag{2.15}$$

As a result, $\{\boldsymbol{g}_k\}$ belong to the null space of $\boldsymbol{A}^*$. Since rank($\boldsymbol{A}$) = n, the dimension of the null space is equal to m-n which is also the dimension of the range space of $\boldsymbol{G}$. Therefore

$$\mathrm{R}(\boldsymbol{G})=N(\boldsymbol{A}^*) \tag{2.16}$$

Since by definition

$$\boldsymbol{S}^*\boldsymbol{G} = 0 \tag{2.17}$$

We have $\mathrm{R}(\boldsymbol{G})=N(\boldsymbol{S}^*)$, hence $N(\boldsymbol{S}^*)=N(\boldsymbol{A}^*)$ Since range space is orthogonal complement to null space,

$$\mathrm{R}(\boldsymbol{A})=\mathrm{R}(\boldsymbol{S}) \tag{2.18}$$

As a result, the DOA's of the signal sources are the only solutions of the equation

$$\boldsymbol{a}^*(\theta,f)\boldsymbol{G}\boldsymbol{G}^*\boldsymbol{a}(\theta,f)=0\,,\qquad m>n \tag{2.19}$$

Since it is easier to search peaks than to search nulls, (2.19) are written as

$$\max_{\{\theta_1,\dots,\theta_n\}}\frac{1}{\boldsymbol{a}^*(\theta,f)\boldsymbol{G}\boldsymbol{G}^*\boldsymbol{a}(\theta,f)}\,,\qquad \text{m>n} \tag{2.20}$$

The range spaces R($\boldsymbol{S}$) and R($\boldsymbol{G}$) are called respectively the signal and noise subspaces.

2.2.2 Root-MUSIC

In Root-Music, the n DOA estimates are found as the angular positions of the n roots of the equation

$$\boldsymbol{a}^T(z^{-1})\boldsymbol{G}\boldsymbol{G}^*\boldsymbol{a}(z)=0\,,\qquad m>n \tag{2.21}$$

which are located nearest the unit circle. e^{-j} is replaced with z.

2.2.3 Min-Norm

MUSIC uses m-n linearly independent eigenvectors of R($\boldsymbol{G}$) to obtain DOA estimation. But it is possible to use only one eigenvector since all vectors are

orthogonal to manifold vector $\{a(\theta_k, f)\}_{k=1}^{n}$. The aim here is to achieve some computational saving without sacrificing the accuracy.

We should find an eigenvector in R($\boldsymbol{G}$) with first element equal to 1, and having minimum Euclidean norm. This eigenvector must satisfy the equation

$$S^* \begin{bmatrix} 1 \\ \boldsymbol{g} \end{bmatrix} = 0 \tag{2.22}$$

We partition the eigenvector matrix $\boldsymbol{S}$ as

$$\boldsymbol{S} = \begin{bmatrix} \alpha^* \\ \overline{\boldsymbol{S}} \end{bmatrix} \tag{2.23}$$

Then (2.22) can be rewritten as

$$\overline{\boldsymbol{S}}^* \boldsymbol{g} = -\alpha \tag{2.24}$$

The minimum norm solution to (2.24) is

$$\hat{\boldsymbol{g}} = -\overline{\boldsymbol{S}}(\overline{\boldsymbol{S}}^* \overline{\boldsymbol{S}})^{-1} \alpha \tag{2.25}$$

Then Min-Norm DOA estimates are determined by

$$\max_{\{\theta_1, \ldots, \theta_n\}} \frac{1}{\left| \boldsymbol{a}^*(\theta, f) \begin{bmatrix} \mathbf{1} \\ \hat{\boldsymbol{g}} \end{bmatrix} \right|^2} \tag{2.26}$$

2.2.4 ESPRIT (Signal Parameters by Rotational Invariance Techniques)

Let

$$\boldsymbol{A}_1 = [I_{m-1} \;\; 0]\boldsymbol{A} \qquad (m\text{-}1)\text{x}n \qquad (2.27)$$

$$\boldsymbol{A}_2 = [0 \;\; I_{m-1}]\boldsymbol{A} \qquad (m\text{-}1)\text{x}n \qquad (2.28)$$

where $\mathbf{I}_{m-1}$ is the identity matrix of dimension (m-1)x(m-1) and $[\mathbf{I}_{m-1} \;\; 0]$ and $[0 \;\; \mathbf{I}_{m-1}]$ are (m-1)xm. It can be verified that

$$\boldsymbol{A_2}=\boldsymbol{A_1 D} \qquad (2.29)$$

where

$$\boldsymbol{D} = \begin{bmatrix} e^{-j2\Pi f\frac{d}{c}\sin(\theta_1)} & \cdots & 0 \\ \vdots & \ddots & \vdots \\ 0 & \cdots & e^{-j2\Pi f\frac{d}{c}\sin(\theta_n)} \end{bmatrix} \qquad (2.30)$$

We define $\boldsymbol{S}_1$ *and* $\boldsymbol{S}_2$ as

$$\boldsymbol{S}_1 = [\boldsymbol{I}_{m-1} \;\; 0]\boldsymbol{S} \qquad (2.31)$$

$$\boldsymbol{S}_2 = [0 \;\; \boldsymbol{I}_{m-1}]\boldsymbol{S} \qquad (2.32)$$

We can write signal subspace eigenvector matrix as

$$\boldsymbol{S} = \boldsymbol{AC} \tag{2.33}$$

$\boldsymbol{C}$ is the nxn nonsingular matrix given by

$$\boldsymbol{C} = \boldsymbol{PA}^{*}\boldsymbol{S}\,\text{Å}^{\circ\,-1} \tag{2.34}$$

where

$$\text{Å} = \begin{bmatrix} \lambda_1 - \sigma^2 & \cdots & 0 \\ \vdots & \ddots & \vdots \\ 0 & \cdots & \lambda_n - \sigma^2 \end{bmatrix} \tag{2.35}$$

By using (2.27), (2.29), and (2.33), we obtain an equation between $\boldsymbol{S_1}$and $\boldsymbol{S_2}$:

$$\boldsymbol{S_2} = \boldsymbol{S_1 C^{-1} D C} = \boldsymbol{S_1}\emptyset \tag{2.36}$$

Since $\boldsymbol{S_1}$and $\boldsymbol{S_2}$ have full column rank, $\emptyset$ has a unique solution given by

$$\emptyset = (\boldsymbol{S_1^{*} S_1})^{-1}\boldsymbol{S_2} \tag{2.37}$$

$\boldsymbol{C^{-1}DC}$ is a similarity transformation so that eigenvalues of $\boldsymbol{D}$ and $\emptyset$ are the same. While the eigenvalues of $\boldsymbol{D}$ are the exponentials seen in (2.30), we can estimate DOA's of signal sources by finding the eigenvalues of $\emptyset$.

CHAPTER 3

DOA ESTIMATION OF WIDEBAND SIGNALS

In this chapter, wideband problem will be introduced, and basic differences between narrowband and wideband signals will be told. Before concentrating on our main wideband method in this thesis, some wideband methods will be given.

3.1 Definition of Wideband Signals

A wideband signal is any signal whose energy is distributed over a bandwidth that is large in comparison to the signal's center frequency.

3.2 Differences Between Wideband and Narrowband Signals

Direct exploitation of an array of raw wideband signals for DOA estimation using traditional narrowband techniques will fail. The narrowband methods exploit the fact that time delays directly translate to a phase shift in the frequency domain.

$$s(t-\tau) \leftrightarrow S(f)e^{-j2\pi \cdot f.\tau} \tag{3.1}$$

Since the phase shift is nearly constant over the bandwidth for narrowband signals, the delayed signal in the time domain can be written as

$$S(f).e^{-j2\pi.f.\tau} \approx S(f).e^{-j.2\pi.f_c.\tau} \leftrightarrow s(t).e^{-j2\pi.f_c\tau} \tag{3.2}$$

where f_c is the center frequency. The phase shift is now independent of time, where the time delay τ is a function of the location of the source relative to the array elements. Let us accept that there are M sensor elements, and P signal sources while M>P. A well-accepted model for the linear array outputs is given by a weighted sum of steering vectors embedded in noise

$$\mathbf{x}(t)=[\mathbf{a}(\theta_0) \ldots \mathbf{a}(\theta_{P-1})]\, \mathbf{s}(t) + \mathbf{n}(t) \tag{3.3}$$

$$\mathbf{a}(\theta_i)= [1\ e^{-j2\pi f_c (d_1/c)\sin\theta_i} \ldots e^{-j2\pi f_c (d_{M-1}/c)\sin\theta_i}]^T \tag{3.4}$$

where $\mathbf{a}(\theta_i)$ is the Mx1 array manifold vector for the *i*th source and **x** is the Mx1 array output vector, **s** is the Px1 signal vector, and **n** is the Mx1 noise vector. In the expression for the array manifold vector, d_m is the sensor displacement of the **m**th element with respect to the first element, c is the speed of propagation, and θ_i is the azimuth angle pointing to the ith source.

For a wideband source, the array output after baseband conversion is no longer constant. Therefore, we can't use (3.4) for array manifold representation. For the wideband case, the array outputs are modeled as, [2]

$$\mathbf{x}(t)= \int X(f) e^{-j2\pi(f-f_c)t}\, df \tag{3.5}$$

where

$$\mathbf{X}(f)=[\mathbf{a}(f,\theta_0) \ldots \mathbf{a}(f, \theta_{P-1})]\, \mathbf{S}(f) + \mathbf{N}(f) \tag{3.6}$$

and

$$\mathbf{a}(f,\theta_i)= [1\ \ e^{-j2\pi f (d_1/c)\sin\theta_i} \ldots e^{-j2\pi f (d_{M-1}/c)\sin\theta_i}]^T \tag{3.7}$$

Figure 3.1 shows the support of ULA output due to two sources, after taking a Fourier transform in both the temporal and spatial domains.

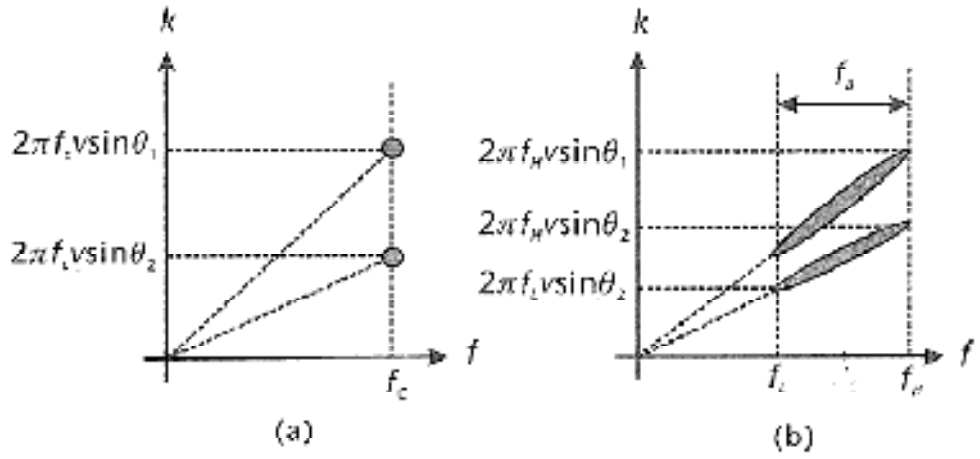

Figure 3.1: Frequency support for the array output, where the horizontal and vertical axes represent temporal and spatial frequencies, respectively, for: (a) two narrowband sources, and (b) two wideband sources, [2]

For the narrowband case shown in figure 3.1(a), the sources are well-separated in the spatial frequency axis. For the wideband case without bandpass filtering shown in figure 3.1(b), the spatial frequency bandwidths overlap so that it is difficult to separate the two sources.

Usually, the array outputs are collected in a sequence of snapshots, where the time interval between snapshots is large enough for the signal amplitudes S(*f*) to decorrelate over time. Therefore, the covariance matrix of the array output at frequency f is modeled as

$$\mathbf{R}(f) = \mathbf{A}(f, \boldsymbol{\theta})\mathbf{R}_s(f)\mathbf{A}^H(f, \boldsymbol{\theta}) + \sigma^2(f)\mathbf{I} \tag{3.8}$$

where

$$\mathbf{A}(f, \theta) = [\mathbf{a}(f,\theta_0) \ldots \mathbf{a}(f, \theta_{P-1})] \tag{3.9}$$

$\mathbf{R}_s(f)$ is the covariance matrix for the signal matrix $\mathbf{S}(f)$, and $\sigma^2(f)$ is the noise variance. The composite covariance matrix for array output $\mathbf{X}(f)$ is

$$\mathbf{R} = \int \mathbf{R}(f)\, df \tag{3.10}$$

For narrowband sources, $\mathbf{R}=\mathbf{R}(f_c)$. The matrix $\mathbf{R}(f)$ has P dominant eigenvalues whose corresponding eigenvectors represent a signal subspace. The remaining M-P eigenvectors represent the noise subspace. However, when the sources are wideband, the number of significant eigenvalues for the covariance matrix is larger than P, due to the mixing of different frequency components. Therefore it is more difficult to distinguish the signal and noise subspaces in wideband rather than in narrowband.

3.3 Introduction to Wideband DOA Estimation Methods

3.3.1 Incoherent Wideband DOA Estimation

The incoherent methods process each frequency bin independently and average the DOA estimates over all the bins. [2] Since each decomposed signal is approximated as a narrowband signal, any narrowband DOA estimation method can be used. For example, when MUSIC is used as the narrowband method, K frequency bins are summed incoherently

$$\hat{\theta} = arg\min_{\theta} \sum_{i=0}^{K-1} \boldsymbol{a}^H(f_i,\theta)\mathbf{W_i}\mathbf{W_i^H}\boldsymbol{a}^H(f_i,\theta) \tag{3.11}$$

where $\mathbf{W_i}$ is the noise subspace, and $\boldsymbol{a}(f_i, \theta)$ is the array manifold at frequency f_i. The noise subspace is usually unavailable.

The incoherent wideband methods provide good DOA estimates in favorable situations, such as high SNR and well-separated source locations. However, when the SNR is low or the noise level is not uniform over frequency bins, it can perform worse than using information in a single frequency bin. Furthermore, when two signals are close to each other, the averaging process could make the estimates worse. When SNR is high, the width of the peaks in MUSIC spectrum become narrow and multiple peaks around the source location can appear when the spectrums for different frequency bins are averaged. As a result, high SNR may not work sometimes when there are more than one source.

3.3.2 Coherent Wideband DOA Estimation

The coherent methods attempt to align the signal subspaces that are associated with the DOA of the sources among all frequency bins. This alignment is accomplished by a transformation of the covariance matrices associated with each bin. After the transformation, the signal and noise subspaces are coherent over the frequency bins, so that the formation of the composite covariance matrix is meaningful.

Three of coherent wideband methods will be explained in this subsection. [2]

3.3.2.1 Coherent Signal Subspace Method (CSSM)

CSSM was introduced by Wang and Kaveh [3]**.** In this method, it was shown that it is possible to combine the signal subspaces in different frequencies to obtain a single common signal subspace with algebraic properties indicative of the number of sources and their angles of arrival. For this, we have the following lemma:

Let's assume we have a uniform linear array with M sensors. Under the condition that $\boldsymbol{A}(f_j), j=1, \ldots, J,$ have a rank of d, there exist nonsingular MxM matrices $\mathbf{T}(f_j)$, $j=1,\ldots,J$ such that

$$\mathbf{T}(f_j)\boldsymbol{A}(f_j)= \boldsymbol{A}(f_0), \quad j=1,\ldots,J \tag{3.12}$$

The proof is simple. Since $\boldsymbol{A}(f_j)$ and $\boldsymbol{A}(f_0)$ have a rank of d, there must exist Mx(M-d) matrices $\boldsymbol{B}(f_j)$ and $\mathbf{B}(f_0)$, such that the MxM matrices $[\boldsymbol{A}(f_j) \mid \boldsymbol{B}(f_j)]$ and $[\boldsymbol{A}(f_0) \mid \boldsymbol{B}(f_0)]$ are nonsingular. An obvious choice for $\mathbf{T}(f_j)$ is then

$$\mathbf{T}(f_j) = [\boldsymbol{A}(f_0) \mid \boldsymbol{B}(f_0)]\, [\boldsymbol{A}(f_j) \mid \boldsymbol{B}(f_j)]^{-1} \tag{3.13}$$

The transformation matrices $\mathbf{T}(f_j)$, j=1,2,…,J are non-unique.

After constructing $\mathbf{T}(f_j)$, an estimate of the composite covariance matrix is formed via

$$\mathbf{R}_{\text{com}}=\sum_{j=0}^{J-1} \alpha_j \mathbf{T}_j \mathbf{R}_j \mathbf{T}_j^H \tag{3.14}$$

where α_j is a weighting.

There are some methods in practice to obtain $\mathbf{T}(f_j)$. Here, one method will be given:

The construction of $\mathbf{T}_j$ requires initial estimates of unknown angles of arrival. We hypothesize that a knowledge of the neighborhoods of these angles is sufficient to effect the advantages of coherent processing. The first step in estimating T is then to perform an initial estimate of AOA's.

Let $\beta_1,\ldots,\beta_d$ be the initial estimates of the angles and $\boldsymbol{A}_\beta(f_j)$, Mxd be the preliminary direction matrix for *j*th narrowband component. Take the estimate of the linear transformation in the form

$$\hat{\mathbf{T}}(f_j) = [\boldsymbol{A}(f_0) \mid \boldsymbol{B}(f_0)]\,[\boldsymbol{A}(f_j) \mid \boldsymbol{B}(f_j)]^{-1}, \quad j=1,\ldots,J \tag{3.15}$$

Solution: $\boldsymbol{B}^{\mathrm{T}}(f_0)=\boldsymbol{B}^{\mathrm{T}}(f_j)=[\boldsymbol{O}_{dx(M-d)} \mid \boldsymbol{I}_{(M-d)}]$. Such a choice offers fast computation since the inversion of the MxM matrix can be obtained by using block matrix inversion formulas, i.e.,

$$\hat{\mathbf{T}}(f_j) = \begin{bmatrix} \boldsymbol{T}_{11} & \boldsymbol{T}_{12} \\ \boldsymbol{T}_{21} & \boldsymbol{T}_{22} \end{bmatrix} \tag{3.16}$$

with

$\mathbf{T}_{11}=\boldsymbol{A}_\beta^{(u)}(f_0)[\boldsymbol{A}_\beta^{(u)}(f_j)]^{-1}$

$\mathbf{T}_{12}=\boldsymbol{O}_{dx(M-d)}$

$\mathbf{T}_{21}=\boldsymbol{A}_\beta^{(l)}(f_0)[\boldsymbol{A}_\beta^{(u)}(f_j)]^{-1} - \boldsymbol{A}_\beta^{(u)}(f_j)[\boldsymbol{A}_\beta^{(u)}(f_j)]^{-1}$

$\mathbf{T}_{22}=\boldsymbol{I}_{M-d}$

where $\boldsymbol{A}_\beta^{(l)}(f)$ and $\boldsymbol{A}_\beta^{(u)}(f)$ are the lower (M-d) x d and the upper d x d block of $\boldsymbol{A}_\beta(f)$.

Once the composite matrix is formed, any narrowband method is applied to the matrix $\mathbf{R}_{com}$ to generate DOA estimates. Compared with the incoherent methods, CSSM has been shown to exhibit lower detection and resolution SNR threshold.

3.3.2.2 Beamforming Invariance Coherent Signal Subspace Method (BICSSM)

BICSSM is introduced in [4]. BICSSM uses a transformation matrix to form the composite covariance matrix and applies a subspace method over the composite matrix like CSSM. Unlike CSSM, the transformation matrices in BICSSM are actually a bank of beamformers tuned to certain look directions.

A designed criterion based on the principles of Least Square fit is employed to construct a beamforming matrix for each of the narrowband frequency bins extracted from the wideband array data. The beamforming matrices perform the same operation as do the focusing matrices in CSSM without knowing the spatial distribution of wideband sources. The idea is to conduct beamspace transformation at each of J frequency bins with the beamforming matrices chosen so that the beam patterns are essentially identical for all frequency bins. For simplicity, consider one beam pattern

$$\boldsymbol{w}(\vec{r}, f_j) = \boldsymbol{w}_j^H \boldsymbol{a}(\vec{r}, f_j) \quad , \quad j=1,\ldots,J \tag{3.17}$$

Where $\boldsymbol{w}_j$ is the Mx1 (M: number of sensors) complex weight vector employed at the jth frequency bin. As an approximation method, we propose a LS fit procedure for constructing weight vectors that nearly produce frequency-invariant beam patterns. The BI weight vectors associated with J frequency bins are then determined by

$$\min_{\boldsymbol{w}_j} \int_{\Omega} \rho(\vec{r}\,) \left| \boldsymbol{w}_0^H a(\vec{r}, f_0) - \boldsymbol{w}_j^H \boldsymbol{a}(\vec{r}, f_j) \right|^2 d\vec{r} \quad , \quad j=1,\ldots,J \tag{3.18}$$

where Ω is the field of view(FOV). Note that f_0 doesn't need to be one of f_j, $j=1,\ldots,J$. The solutions to (3.18) are given by

$$\boldsymbol{w}_j = \mathbf{U}_j^{-1}\mathbf{S}_j\boldsymbol{w}_0 \quad , \quad j=1,\ldots,J \tag{3.19}$$

Where

$$\mathbf{U}_j = \int_\Omega \rho(\vec{r})\boldsymbol{a}(\vec{r},f_j)\boldsymbol{a}^H(\vec{r},f_j)d\vec{r} \quad , \quad j=1,\ldots,J \tag{3.20}$$

$$\mathbf{S}_j = \int_\Omega \rho(\vec{r})\boldsymbol{a}(\vec{r},f_j)\boldsymbol{a}^H(\vec{r},f_0)d\vec{r} \quad , \quad j=1,\ldots,J \tag{3.21}$$

The transformation matrix for the jth frequency bin is

$$\mathbf{W}_j = [\boldsymbol{w}_{j,0} \quad \ldots \quad \boldsymbol{w}_{j,N-1}]^H \tag{3.22}$$

where N is the number of look directions in FOV. If there are D sources, N is chosen to be such that $D \le N < M$.

BICSSM removes the need to estimate focusing angles by attempting to cohere the transformed steering matrices within a FOV. Since $\mathbf{W}_j\mathbf{a}(f_j, \Theta) = \mathbf{W}_0\mathbf{a}(f_0, \Theta)$ in FOV, the composite covariance matrix is

$$\mathbf{R}_{com} = \mathbf{B}(f_0)\,\mathbf{R}_s\,\mathbf{B}(f_0)^H \tag{3.23}$$

$$\mathbf{R}_s = \sum_{j=0}^{J-1}\alpha_j\mathbf{R}_s(f_j) \tag{3.24}$$

where α_j is a set of preselected weights. α_j can be chosen to be α_j=1 , $j=1,\ldots,J$. After constructing the composite covariance matrix, any narrowband method can be applied to estimate DOAs.

3.3.2.3 Weighted Average of Signal Subspaces for Robust Wideband Direction Finding (WAVES)

The WAVES method is introduced in [5]. It uses a pseudo data matrix that is inspired by the weighted subspace fitting (WSF) method [6]. Specifically, WAVES estimates the noise subspaces at a reference frequency by taking a singular value decomposition of the pseudo data matrix **Z**,

$$\mathbf{Z}= [\mathbf{T_0F_0P_0} \quad \mathbf{T_1F_1P_1} \ \ldots \ \mathbf{T_{K-1}F_{K-1}P_{K-1}}] \tag{3.25}$$

where $\mathbf{T_i}$ is the focusing matrix, and $\mathbf{F_i}$ is the signal subspace at frequency f_i. The focusing matrix matrix $\mathbf{T_i}$ is obtained using focusing angles or via BICSSM. The matrix $\mathbf{P_i}$ is a diagonal weighting matrix. The kth diagonal element of the weighting matrix $\mathbf{P_i}$ is

$$[\mathbf{P_i}]_{(k,k)} = \frac{\lambda_{i,k}-\sigma_n^2}{\sqrt{\lambda_{i,k}\sigma_n^2}} \tag{3.26}$$

where $\lambda_{i,k}$ is the kth largest eigenvalue of $\mathbf{R}_i$, and σ_n^2 is the noise power, which is assumed to be a constant over all the frequency bins. WAVES determines the noise subspace U_N, which is M x (K-1)P matrix via the singular value decomposition of the M x KP pseudo data matrix

$$\mathbf{Z} = [\mathbf{U}_s \ \mathbf{U}_N] \begin{bmatrix} \mathbf{\Sigma_S} & 0 \\ 0 & \mathbf{\Sigma_N} \end{bmatrix} \begin{bmatrix} \mathbf{V}_S^H \\ \mathbf{V}_N^H \end{bmatrix} \tag{3.27}$$

Finally, the MUSIC algorithm is applied with the noise subspace $\mathbf{U}_N$.

3.3.3 Array Interpolation

This method is told in [7]. A set of virtual arrays is generated, each for a different frequency band, having the same array manifold by using an interpolation technique. The covariance matrices of these arrays are added up to produce a composite covariance matrix.

Consider a planar array with sensors located at coordinates $\{x_i, y_i\}$. The response of this array to a narrowband signal at frequency f_0 is the same as the response of an array with sensors located at coordinates $\{\alpha.x_i, \alpha.y_i\}$ to the narrowband signal at frequency f_0 / α . We can use this property for wideband signals: Consider a wideband signal divided into multiple narrow bands with center frequencies f_k. Assume that each band is received by a different array, where all the arrays is stretched or compressed versions of a nominal array to have the same response. Because all arrays have the same response, it is possible to combine the covariance matrices for the different frequencies by simple addition.

In this method, we have only a single array, not a collection of arrays tuned to different frequencies. However, we use virtual arrays whose outputs are obtained by a simple interpolation technique. The design of the interpolator needs to be performed only once, off-line, and thus does not impose a computational burden.

Assume, for a moment, that we use different arrays for collecting data at different frequencies. The data covariance covariance matrix of the lth array is

$$\overline{\mathbf{R}}_l = \overline{\mathbf{A}}(w_l)\,\mathbf{R}_s(w_l)\,\overline{\mathbf{A}}^H(w_l) + \overline{\mathbf{R}}_v(w_l) \tag{3.16}$$

where $\mathbf{A}^{\mathrm{H}}(w_l)$ is the array manifold of the lth array at frequency w_l, $\mathbf{R}_{\mathrm{s}}(w_l)$ is the the signal covariance matrix, and $\mathbf{R}_{\mathrm{v}}(w_l)$ is the noise covariance of this array. By design, we can make all these array manifolds equal,

$$\bar{\boldsymbol{A}}(w_l) = \bar{\boldsymbol{A}} \tag{3.17}$$

The composite covariance matrix is then the sum of the covariance matrices of the different arrays,

$$\bar{\mathbf{R}} = \sum_{l=1}^{L} \bar{\mathbf{R}}_l = \bar{\mathbf{A}} \bar{\mathbf{R}}_s \bar{\mathbf{A}} + \bar{\mathbf{R}}_n \tag{3.18}$$

where

$$\bar{\mathbf{R}}_s = \sum_{l=1}^{L} \mathbf{R}_{\mathrm{s}}(w_l) \tag{3.19}$$

$$\bar{\mathbf{R}}_n = \sum_{l=1}^{L} \mathbf{R}_{\mathrm{v}}(w_l) \tag{3.20}$$

The interpolated array approach is based on the idea that the array manifold of a virtual array, whose element locations are chosen by the user, can be obtained by linear interpolation of the array manifold of the real array within a limited sector in field of view (FOV):

$$\mathbf{B}.\mathbf{a}(\theta) = \bar{\mathbf{a}}(\theta) \tag{3.21}$$

where $\mathbf{a}(\theta)$ is the real array manifold and $\bar{\mathbf{a}}(\theta)$ is the virtual array manifold. In practice, the field of view will be divided into several sectors, and a different interpolation matrix will be calculated for each sector. To simplify the discussion, a single sector is considered here.

In the context of wideband problem, if we denote the real array manifold at w_l by $\mathbf{a}_l(\theta)$,

$$\mathbf{B}_l.\ \mathbf{a}_l(\theta) = \bar{\mathbf{a}}(\theta) \tag{3.22}$$

In other words, for each frequency we need to compute a single interpolation matrix which maps the real array manifold to a fixed array manifold, for a given sector. Given the interpolation matrix $\mathbf{B}_l$ we can compute the covariance matrix $\bar{\mathbf{R}}_l$ of the virtual array from the covariance matrix $\mathbf{R}$ of the real array:

$$\bar{\mathbf{R}}_l = \mathbf{B}_l \mathbf{R} \mathbf{B}_l^H \tag{3.23}$$

We choose the virtual arrays to be ULA for simplicity, but any type of array can be chosen as virtual arrays. The physical arrays are arbitrary. The ULA manifold with omni-directional sensors is given by

$$\bar{\mathbf{a}}(\theta) = \left[1, e^{j2\pi(d/\lambda)\sin\theta}, \ldots, e^{j2\pi(d/\lambda)(M-1)\sin\theta}\right]^T \tag{3.24}$$

where λ is the wavelength of the received signals, and d is the element spacing. Since

$$\mathrm{d}/\lambda = \mathrm{d}\frac{w}{2\pi c} \tag{3.25}$$

If we select the element spacing according to the rule

$$dw = \text{constant} \tag{3.26}$$

Then, the array manifold will be the same for every frequency. Therefore, the interpolated arrays are chosen as follows:

$$d_l = \frac{d_0 w_0}{w_l} \tag{3.27}$$

where d_l is the element spacing for the interpolated array at frequency w_l, and d_0 is the element spacing at the center frequency w_0. Thus

$$\mathbf{A} = \mathbf{B}_l \mathbf{A}(w_l) \ , \quad \forall l \tag{3.28}$$

Since all the arrays have the same manifold and therefore the same direction matrix, we can obtain the composite matrix via

$$\mathbf{R} = \sum_{l=1}^{L} \overline{\mathbf{R}}_l = \sum_{l=1}^{L} \mathbf{B}_l \mathbf{R}_l \mathbf{B}_l^H \tag{3.29}$$

This method may face numerical stability problems due to ill conditioned transformation matrices.

3.3.4 Method Based On Frequency Invariant Beamforming

This method is studied in detail in the next chapter.

CHAPTER 4

FREQUENCY INVARIANT BEAMFORMING METHODS

In this chapter, the main method of interest, i.e. frequency invariant beamforming methods, will be introduced. The aim of the method is to obtain an overall beampattern which doesn't change for different frequencies in the frequency band for which the array is designed.

4.1 Frequency Invariant Beamforming Methods

4.1.1 Chou's Method

The goal of this approach is to use fewer number of sensors than those required by uniformly spaced arrays. [8] There exists a compound array consisting of a set of nested subarrays, each of which is designed for a single frequency band. The most common compound array is shown in Figure 4.1. The bottom subarray has N elements spaced at

$$d = \frac{\lambda_u}{2} \tag{4.1}$$

where λ_u is the wavelength at the highest frequency.

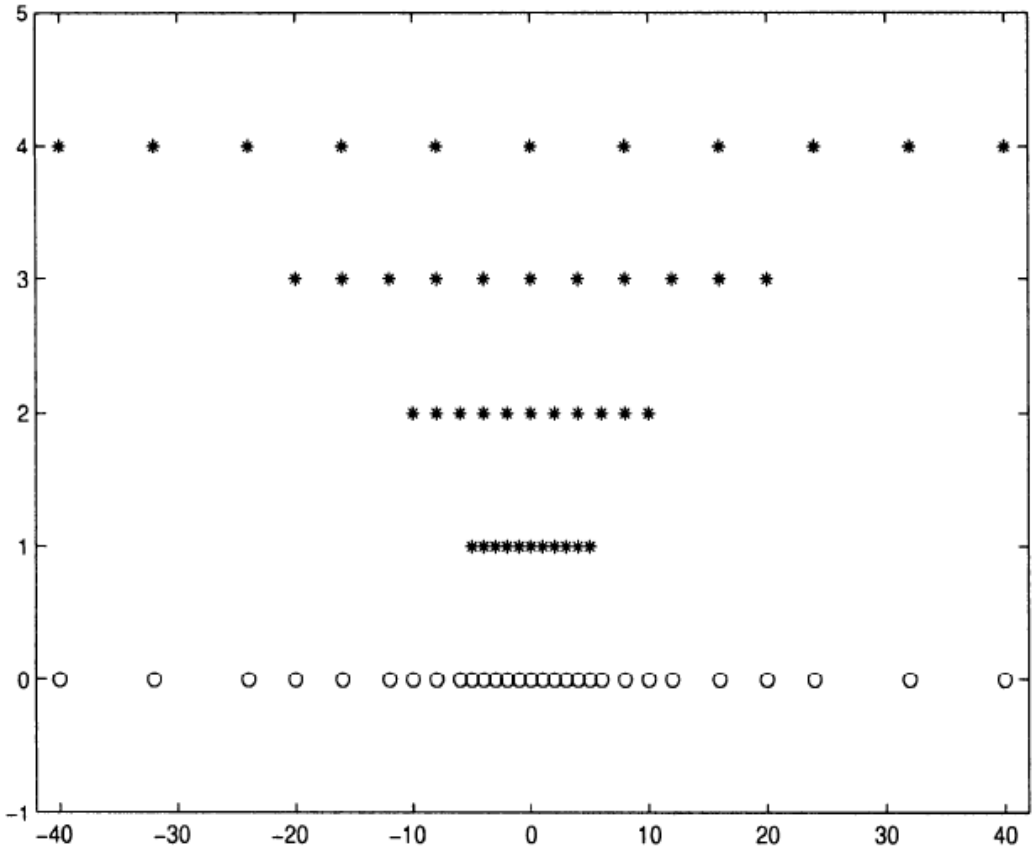

Figure 4.1: Compound array consisting of nested subarrays, [15]

The next subarray has N elements spaced at d= λ_u . The total number of elements is, [15]:

$$N_T = N + 3\left(\frac{N+1}{2}\right), \quad N \text{ odd} \tag{4.2}$$

$$N_T = N + 3\frac{N}{2}, \quad N \text{ even} \tag{4.3}$$

Here N is related with mainlobe beamwidth. If we require that the width of the mainlobe be constant over a frequency band of interest, then the number of elements in that band must be

$$N = \left(\frac{2\alpha}{BW_{NN}} \right) \frac{\lambda_l}{\lambda_u} \tag{4.4}$$

where α is a constant dependent on the shading and BW_{NN} is the beamwidth of the mainlobe. The number of elements of all nested subarrays will be calculated with (4.4).

A different octave band is processed with each subarray; the highest octave $f_u/2<f<f_u$ is processed with the first subarray (the subarray with the closest sensors in Figure 4.1), the next octave with the next subarray, and so forth. Each octave is divided into K bins, where the frequency bins are centered at

$$f_c = f_l \left(1 + \frac{2k+1}{2K} \right) \quad k=0,\ldots,K\text{-}1 \tag{4.5}$$

f_l: Lower frequency of each octave band

We first define a desired beam pattern for a uniform linear array designed at

$$d = \frac{\lambda_u}{2} \tag{4.6}$$

and

$$\lambda_l = 2\lambda_u \tag{4.7}$$

For each of the frequencies in (4.5) , the beam pattern is sampled at

$$u_n = \frac{c}{N_0 df_k} n \quad , \quad -\frac{N_0 - 1}{2} < n < \frac{N_0 - 1}{2} \text{, } N_0 \text{ odd, } 1 \le k \le K \tag{4.8}$$

Then, IDFT is performed on the samples to obtain the weightings in the frequency bin f_k. At last we take DFT to obtain the beam pattern for the corresponding frequency bin.

The compound array approach has two problems. First, frequency dependent amplitude shading which accurately interpolates the subarray properties is very difficult to achieve. Second, we process each subarray in octave bands so that only a very limited set of band ratios is achievable in the case of equally spaced subarrays, i.e. band ratios of 2, 4, 8, and 16 are achievable but band ratios of 6 or 10 are not.

4.1.2 Doles & Benedict's Method

The asymptotic theory of unequally spaced arrays is used to derive relationships between beam pattern properties and array properties; these relationships are used to translate beam pattern requirements into functional requirements on sensor spacings and amplitude shadings; and, the functional requirements are then used to derive a broadband array design. [9] The method told here translates requirements of broadbanding problem into functional requirements on sensor spacings and amplitude shadings.

The array response of a linear array of N+1 omni-directional sensors is given by,

$$A(\xi;\lambda) = \sum_{n=0}^{N} w_n(\lambda)\, exp\{j2\pi\xi\lambda^{-1}x_n\} \tag{4.9}$$

where x_n are the sensor coordinates, $w_n(\lambda)$ are wavelength dependent shading amplitudes, and

$$\xi = \sin\theta - \sin\phi \tag{4.10}$$

where θ is the bearing of the plane wave arrival and ϕ is the beam bearing both measured with respect to broadside. We will extend the coordinates and shading amplitudes to continuous functions *X(v)* and *W(v;λ)* :

$$A(\xi;\lambda) = \sum_{n=-\infty}^{+\infty} G(n,\xi;\lambda) \tag{4.11}$$

where

$$G(v,\xi;\lambda) = W(v;\lambda)\exp\{2\pi j\xi\lambda^{-1}X(v)\} \tag{4.12}$$

Over the interval from 0 to N and $G(v,\xi;\lambda) = 0$ when v is outside this interval. When using the Poisson summation formula in (4.11)

$$A(\xi;\lambda) = \sum_{m=-\infty}^{+\infty} F(m,\xi;\lambda) \tag{4.13}$$

where

$$F(\mu,\xi;\lambda) = \int_{-\infty}^{+\infty} G(v,\xi;\lambda)e^{-2\pi j\mu v}dv \tag{4.14}$$

The asymptotic theory of unequally spaced arrays results from estimating the functions $F(\mu,\xi;\lambda)$.

Here we will consider only end tapered arrays and shading schemes with real coefficients. End tapered means that spacing function $S(v) = X'(v)$ satisfies the condition

$$S'(v) = X''(v) \geq 0 \tag{4.15}$$

(4.15) means that the sensor spacings should be monotonic increasing. Since the coefficients $w_n(\lambda)$ are real, the array response satisfies

$$A^*(\xi,\lambda) = A(-\xi,\lambda) \tag{4.16}$$

As a result, we can carry the analysis only for the interval $0 \le \xi \le 2$.

In the asymptotic theory, there are four basic relationships between beam pattern properties and the two array properties, spatial tapering and amplitude shading. These relationships are the aperture shading conditions and the amplitude shading conditions that are given in Appendix A. These relationships are used to derive the broadband array design criteria, and these derivations are also given in Appendix A.

By considering the broadband beam pattern requirements, the sensor spacings and the amplitude shadings are

$$X(v) = \begin{cases} (\lambda_u/2)v, & 0 \le v \le v^* = P/\beta \\ (P/\beta)(\lambda_u/2)r^{v-v^*}, & v^* = P/\beta \le v \le N \end{cases} \tag{4.17}$$

$$W(v;\lambda) = \begin{cases} S(v)/(\lambda/2), & 0 \le v < S^{-1}(\lambda/2) \\ 1, & S^{-1}(\lambda/2) \le v \le S^{-1}(\beta\lambda/2) \\ 0, & S^{-1}(\beta\lambda/2) < v \le N \end{cases} \tag{4.18}$$

The aperture *P,* the largest spacing β and the design band ratio f_u / f_L are related to the total number of sensors by the equation

$$N = (P/\beta)\ln(e\beta f_u / f_L) \tag{4.19}$$

4.1.3 Ward & Kennedy' s Method

The frequency invariant beam pattern property is defined in terms of a continuously distributed sensor, and the problem of designing a practical sensor array is then treated as an approximation to this continuous sensor using a discrete set of filtered broadband omni-directional array elements. [10], [11] As a result, the problem of designing a broadband array is reduced to one of providing an approximation to a theoretically continuous sensor.

The design method can be used with any one-,two-, and three-dimensional sensor arrays and with any desired beam shape while Doles & Benedict's method is based on a single-sided uniform aperture distribution and a linear array, gives no insight into the problem of designing double-sided or higher dimensional arrays with arbitrary aperture distributions. The locations of sensors are not crucial for our design since the filter responses are designed with respect to sensor spacings. However, we use non-uniform sensor spacings to avoid spatial aliasing and minimize the number of sensors.

To obtain an identical beam pattern at k different frequencies would require a compound array of k subarrays and these k subarrays would be identical if spatial coordinates were expressed in terms of wavelengths. As a result, to produce a frequency invariant beam pattern over a continuous frequency band requires infinite number of subarrays. We must thus emphasize that obtaining a strictly frequency invariant beam pattern from a discrete sensor array is impossible. It is thus necessary to initially consider the concept of a continuous sensor to develop a FI broadband theory.

The output of a one-dimensional continuous sensor is

$$Z_f = \int_{-\infty}^{+\infty} S(x,f)\rho(x,f)dx \tag{4.20}$$

where S: $\mathbf{RxR}^+ \rightarrow \mathbf{C}$ is the signal received at a point x on the sensor due to a signal of frequency f, and ρ: $\mathbf{RxR}^+ \rightarrow \mathbf{C}$ defines the sensitivity distribution of the sensor at a point x and for a frequency f. When the incoming signal is a plane wave the signal received is given by

$$S(x,f) = e^{j2\pi c^{-1} f x \sin(\theta)} \tag{4.21}$$

where c is the speed of wave propagation. With $S(x,f)$ thus defined, the output of the sensor is a function of Θ and can be interpreted as the sensor beam pattern:

$$b_f(\theta) = \int_{-\infty}^{+\infty} e^{j2\pi c^{-1} f x \sin(\theta)} \rho(x,f) dx \tag{4.22}$$

In order for the continuous sensor to be FI, the continuous sensor beam pattern should prove that $b_f(\theta) = b(\theta)$. We now come to our first result: The sensitivity distribution of a sensor can be written as

$$\rho(x,f) = f\ G(xf) \quad , \ \forall f > 0 \tag{4.23}$$

The far-field beam pattern $b_f(\theta)$ will be frequency invariant, i.e.

$$b_f(\theta) = b(\theta) = \int_{-\infty}^{+\infty} e^{j2\pi c^{-1} \xi \sin(\theta)} G(\xi) d\xi \tag{4.24}$$

where G: $\mathbf{R} \rightarrow \mathbf{C}$ is an arbitrary absolutely complex function. We will name G as the primary filter in our broadband design method, the primary filters will give us the ability to obtain any desired beam pattern. Let $b(\theta)$ be an arbitrary continuous

square-integrable FI far-field beam pattern specified for $\theta \in$ **(-π**/2, **π**/2**)**. Then the primary filter generally should satisfy the conditions

$$\Gamma(s) = B(s) = b[sin^{-1}(sc)]\,, \qquad s \in \left(-\frac{1}{c}, \frac{1}{c}\right) \tag{4.25}$$

$$\Gamma(s) = A(s)\,, \quad s \notin \left(-\frac{1}{c}, \frac{1}{c}\right) \tag{4.26}$$

where c is the speed of wave propagation and A(.) is an arbitrary square-integrable function such that

$$A\left[\frac{(-1)^i}{c}\right] = \lim_{s \to \frac{(-1)^i}{c}} B(s) \quad \text{for i=0,1} \tag{4.27}$$

After giving sufficient properties for one-dimensional sensor, we can consider the situation for two-dimensional sensor. The signal received from plane waves by two-dimensional sensor is

$$S(x, f) = e^{j2\pi c^{-1} f(\, x_1 sin\emptyset\, cos\theta + x_2 sin\emptyset\, cos\theta\,)} \tag{4.28}$$

where **x**=(x_1,x_2) is a point on the sensor, $\emptyset$ is the elevation angle and θ is the azimuth angle of the plane wave. Then the beam pattern of the FI two-dimensional sensor is given by

$$b(\emptyset, \theta) = \iint_{-\infty}^{\infty} e^{j2\pi c^{-1}(\, f x_1 sin\emptyset\, cos\theta + f x_2 sin\emptyset\, sin\theta\,)} \times f^2 G(\, x_1 f, x_2 f\,) dx_1 dx_2$$

$$= \iint_{-\infty}^{\infty} e^{j2\pi c^{-1}(\, \xi_1 sin\emptyset\, cos\theta + \xi_2 sin\emptyset\, sin\theta\,)} \times G(\, \xi_1, \xi_2\,) d\xi_1 d\xi_2 \;, \forall f > 0 \tag{4.29}$$

where $\xi_1 = x_1 f, \quad \xi_2 = x_2 f$.

We can generalize the broadband condition for multi-dimensional continuous sensors. A D-dimensional continuous sensor has a frequency invariant far-field beam pattern if

$$\rho(x, f) = f^D G(xf), \quad \forall f > 0 \tag{4.30}$$

where $\boldsymbol{x}$ is a point on the D-dimensional continuous sensor. Then the design of primary filters remains only. The primary filters are expressed in two equivalent representations:

$$G(xf) = A_f(x) = H_x(f), \quad \forall x, \quad f > 0 \tag{4.31}$$

where $A_f: R^D \to C$ is the aperture distribution, $H_{\boldsymbol{x}}: R^+ \to C$ is the primary frequency response. In the scalar version, $G(\boldsymbol{x}f)$ is a symmetric function of spatial variable $\boldsymbol{x}$ and of frequency variable f. This means that f and $\boldsymbol{x}$ can be interchanged without affecting the value of the function. This can be interpreted that $G(\boldsymbol{x}f)$, which appears in (4.23), looks the same if we vary f while holding $\boldsymbol{x}$ fixed, or vary $\boldsymbol{x}$ while holding f fixed. In other words, the primary filter takes the same shape as the aperture distribution. The correspondence between aperture distribution and primary filter response is for both magnitude and phase.

All primary filter responses in a FI broadband sensor for a given $\boldsymbol{x}$ are identical up to a frequency dilation. The proof is simple: Consider the filter response at a point γx where $\gamma>0$, which lies on the radial line from the origin through $\boldsymbol{x}$. Then

$$H_{\gamma x}(f) = G(f\gamma \boldsymbol{x}) = H_{\boldsymbol{x}}(\gamma f) \tag{4.32}$$

which is a dilation property.

Having developed the theory of a broadband FI continuous sensor, we can describe the implementation of a broadband FI array. Let this array have a finite set of identical, discrete, omnidirectional sensors. This array of sensors can only approximate the ideal broadband continuous sensor. For a one-dimensional array, we express this approximation numerically as

$$\tilde{Z}_f = f \sum_{i=0}^{N-1} g_i S(x_i, f) G(x_i f)\,, \qquad \forall f \in (f_L, f_U) \tag{4.33}$$

$$= f \sum_{i=0}^{N-1} g_i H_i(f) e^{j2\pi f x_i c^{-1} \sin\theta}\,, \qquad \forall f \in (f_L, f_U)$$

where g_i is a frequency-independent weighting function to compensate for the possibly nonuniform sensor locations and is told in [9] how to be obtained for the case corresponding to the trapezoidal integration method.

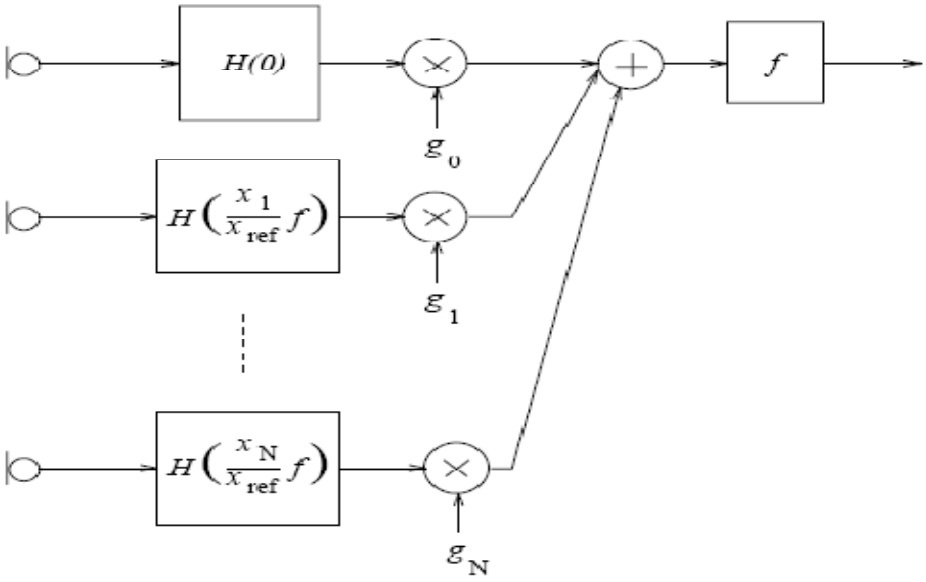

Figure 4.2: Block diagram of a general linear FIB

In Figure 4.2, *H(f)* is the primary filter response at some reference location x_{ref}. Note that the filter response of the zeroth sensor is constant. The sensor locations will be determined by the method developed by Doles and Benedict [9] so that the number of sensors will be minimized while avoiding spatial aliasing. For a linear array, the sensor locations are

$$x_n = \begin{cases} \frac{\lambda_U}{2} n\,, & 0 \le n \le P \\ P\frac{\lambda_U}{2}\left(\frac{P}{P-1}\right)^{n-P}\,, & P < n \le N \end{cases} \tag{4.34}$$

where $P \in \mathbf{N}$ is the aperture length measured in half wavelengths, λ_U is the wavelength for the upper frequency, and $N = P + 1 + \left\lfloor \frac{\ln \frac{f_U}{f_L}}{\ln \frac{P}{P-1}} \right\rfloor$.

The primary filters will have the required dilation property if the *n*th primary filter response is given by

$$H_n(f) = \sum_{k=-(L-1)/2}^{(L-1)/2} h_{ref}[k] e^{-j2\pi f T_n k} \tag{4.35}$$

where $T_n = T\frac{x_n}{x_{ref}}$ is the sampling period of the *n*th sensor. With the substitution $\rho(x,f) = f\,G(xf)$ and the change of variables $u = c^{-1}sin\theta$ and $y = xf$ in (4.22), the Fourier transform relationship between the desired response and the aperture distribution is obvious. Given a desired beam pattern in $u \in [-1/c, 1/c]$, the primary filter response at *x*=1 is

$$\widetilde{H}_1(f) = \int_{-1/c}^{1/c} r_d(u) e^{-j2\pi f u}\, du \tag{4.36}$$

The coefficients for this primary filter can be calculated by direct sampling:

$$h_1[k] = r_d(kT) \tag{4.37}$$

where *T* is the sampling period. According to the dilation property, the coefficients of the reference primary filter are found by

$$h_{ref}[k] = \frac{1}{x_{ref}} r_d\left(\frac{kT}{x_{ref}}\right), \quad x_{ref} > 0 \tag{4.38}$$

All other primary filter responses can be found from the reference primary filter coefficients by using (4.35).

4.2 Performance of the FIB Methods

In this section, we will investigate the performance of three FIB methods: Chou's method, Doles' & Benedict's method, and Ward's & Kennedy's method.

4.2.1 Chou's Method

The performance of Chou's method will be qualified with respect to two criteria:

4.2.1.1 How much the method is successful in obtaining a frequency invariant beam pattern?

Constant parameters: $f_L = 1\,\text{GHz}$, $f_U = 16\,\text{GHz}$

N: Number of sensors

K: Number of frequency bins in each octave

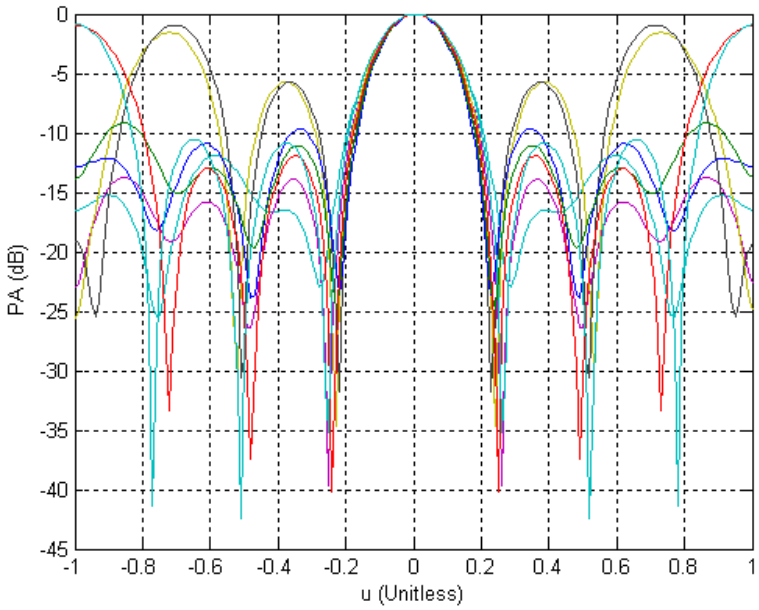

Figure 4.3: The output of the beamformer for K=8 and N=8

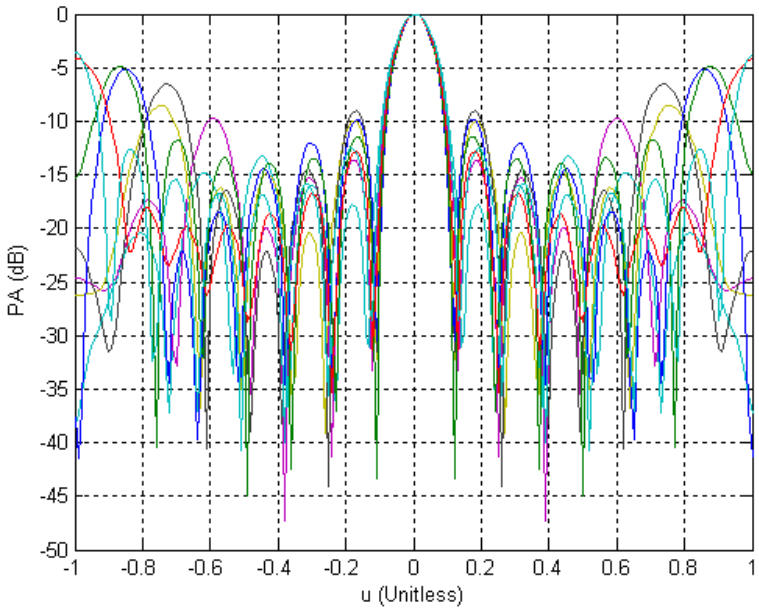

Figure 4.4: The output of the beamformer for K=8 and N=16

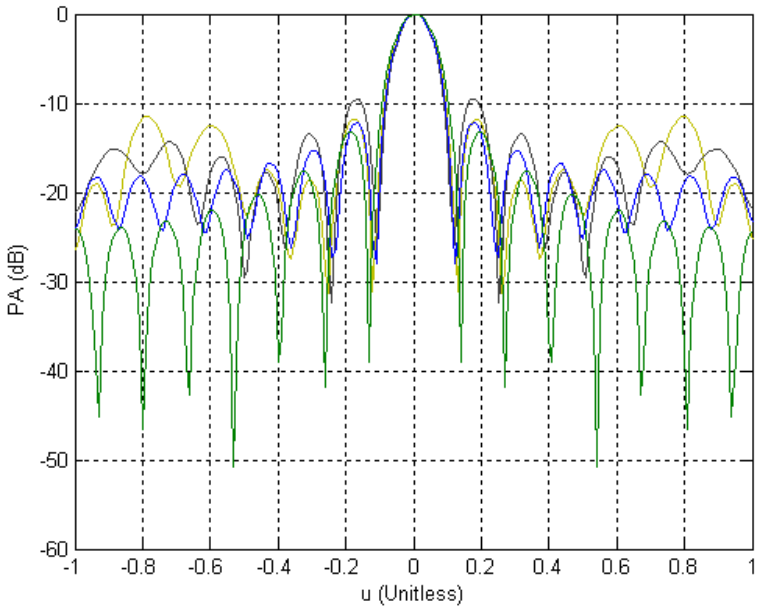

Figure 4.5: The output of the beamformer for K=4 and N=16

As can be seen in fig. 4.3, 4.4, and 4.5, increasing the number of sensors results a better frequency invariancy. And there is no effect of the number of frequency bins

in each octave on the performance, because sensor spacing design is done with respect to lower and upper frequency of an octave band.

4.2.1.1.1 How much the method is successful in estimating the desired beam pattern?

Constant parameters: $f_L = 1\,\text{GHz}$
$f_U = 16\,\text{GHz}$

N: Number of sensors

K: Number of frequency bins in each octave

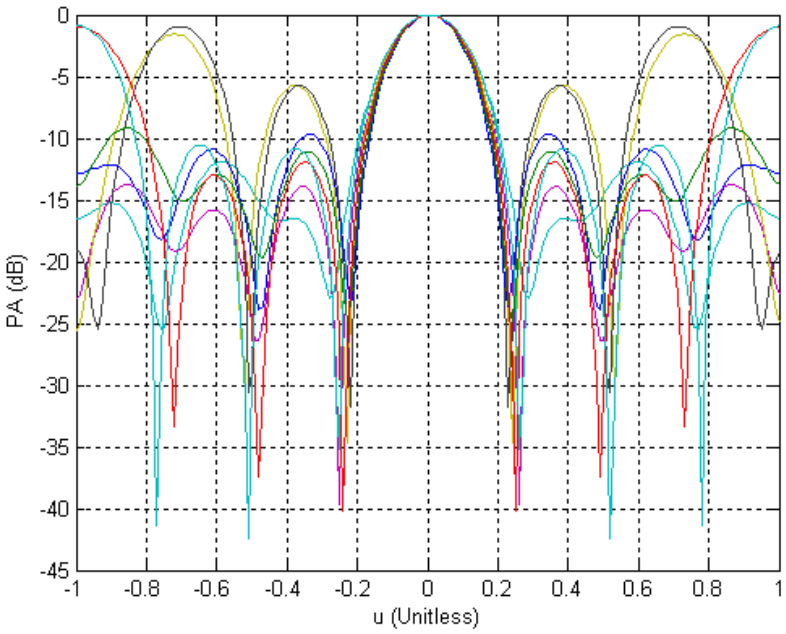

Figure 4.6: The output of the beamformer for K=8 and N=8

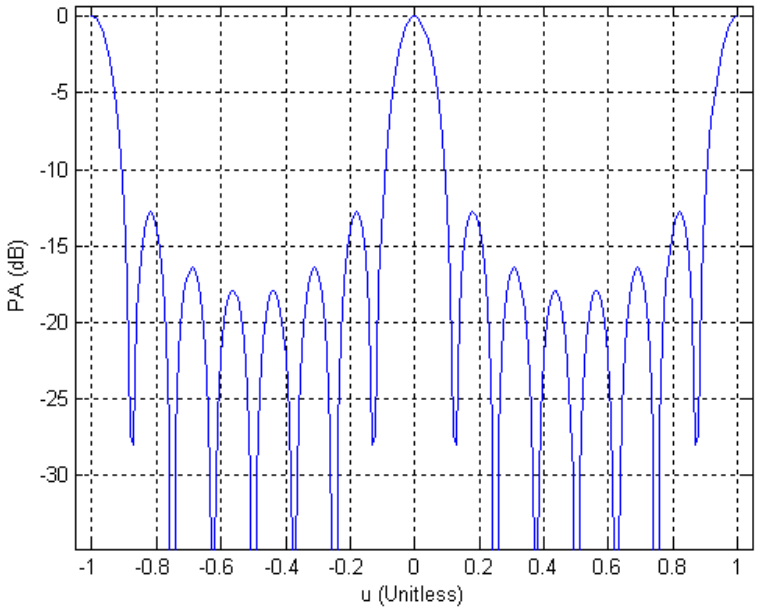

Figure 4.7: The desired beampattern for N=8

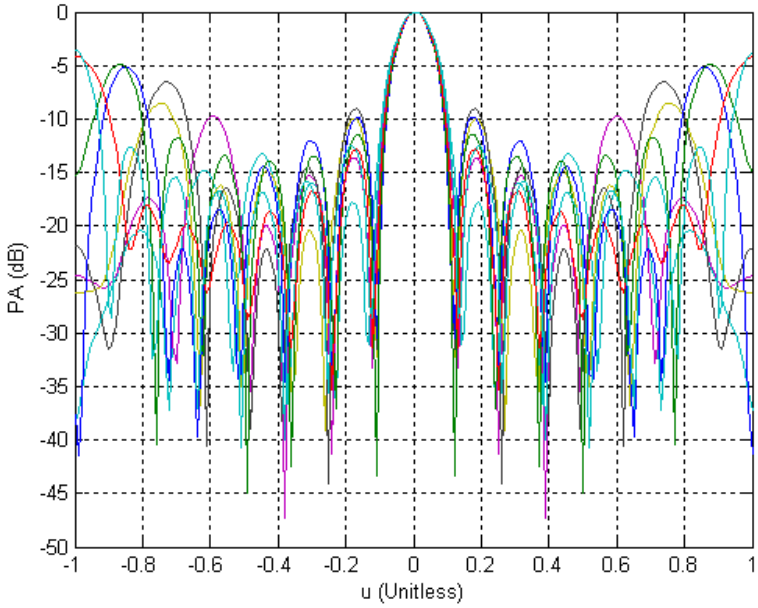

Figure 4.8: The output of the beamformer for K=8 and N=16

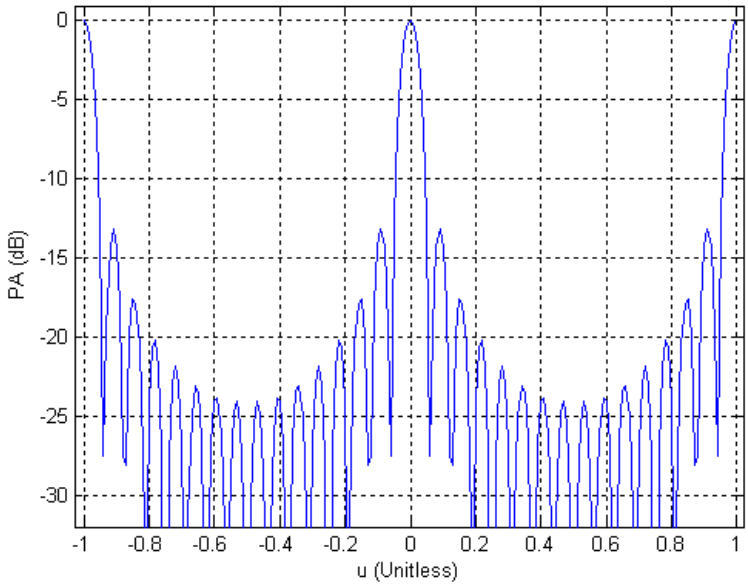

Figure 4.9: The desired beampattern for N=16

Fig. 4.6, 4.7, 4.8, and 4.9 tell us that the number of sensors have little effect on the performance of obtaining the desired beam pattern. More importantly, we should increase the sampling rate to obtain a better estimate of the desired beampattern.

Note that Chou's method can work with any desired beam pattern, but it can only work in octave frequency bands.

4.2.2 Doles' & Benedict's Method

The performance of the method will be qualified with respect to two criteria:

4.2.2.1 How much the method is successful in obtaining a frequency invariant beam pattern in any frequency band?

In order to evaluate the first performance criterion, simulations are done for different aperture lengths. In these simulations, the operating frequency is changed while the frequency band is held constant.

Constant parameters: $\begin{matrix} f_L = 2\ GHz \\ f_U = 18\ GHz \end{matrix}$, $\beta = \frac{1}{2}$

$$N\ (num\ of\ sensors) = \left({}^{P}/_{\beta}\right) \ln\left\{e\beta\left({}^{f_U}/_{f_L}\right)\right\} = \ 2P * \ \ln\{9e\beta\}$$

P: Aperture length

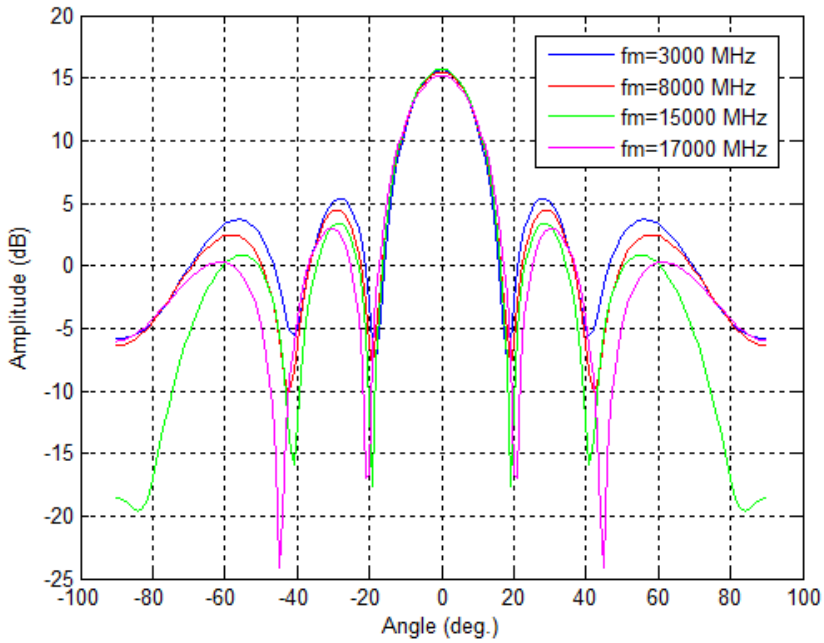

Figure 4.10: Obtained beam patterns for aperture length P=5* $\frac{\lambda_L}{2}$ and N=15

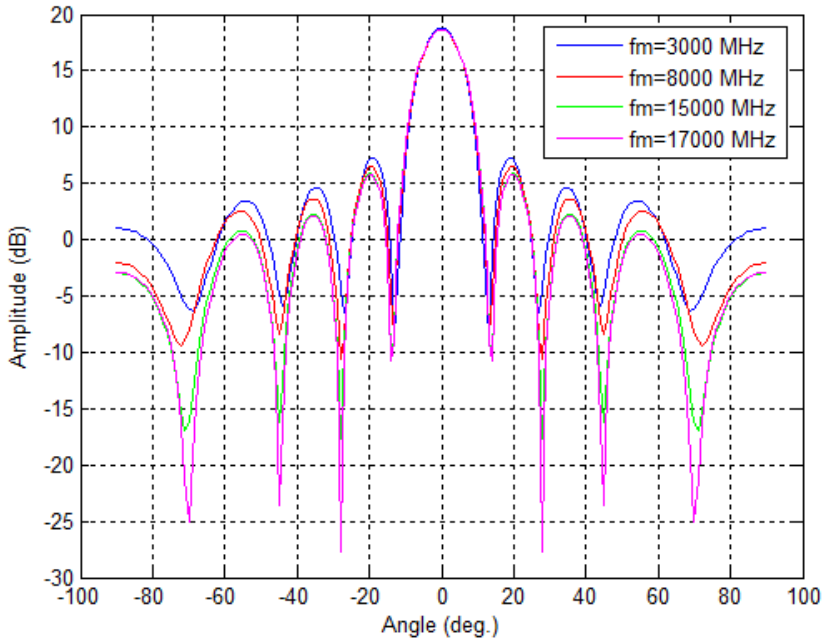

Figure 4.11: Obtained beam patterns for aperture length P=8* $\frac{\lambda_L}{2}$ and N=25

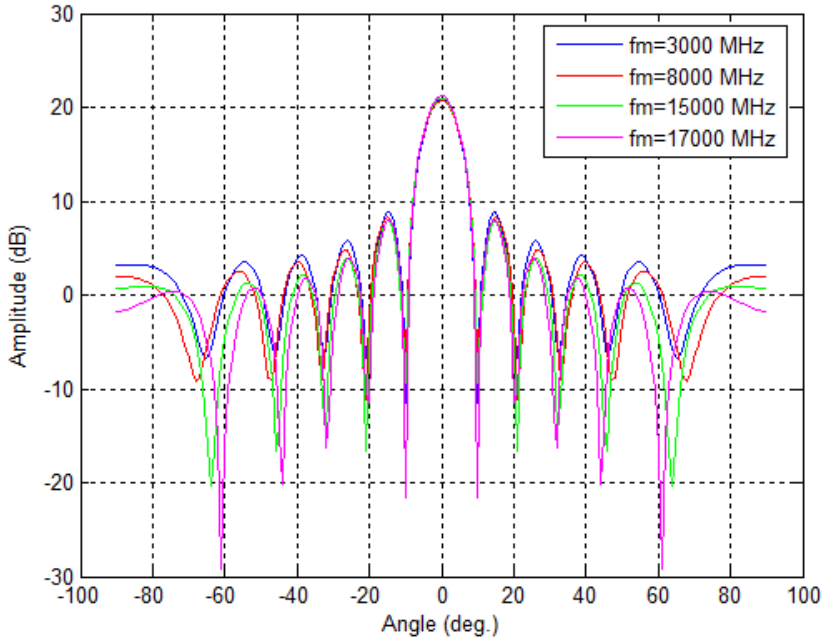

Figure 4.12: Obtained beam patterns for aperture length P=10* $\frac{\lambda_L}{2}$ and N=31

When increasing the aperture length, the number of sensors used increases as a natural result of the method. Using more sensors results more invariant mainlobe with respect to frequency. Note that, the degradation from invariancy increases when propagating from aperture center to aperture edges.

4.2.2.2 How much the method is successful in obtaining desired beam pattern at any operating frequency?

Again, simulations were done for different aperture lengths. In these simulations, both the operating frequency and the frequency band were held constant.

Constant parameters: $f_L = 2\ GHz$, $f_U = 18\ GHz$, $\beta = \frac{1}{2}$, $f_m = 8\ GHz$

$$\text{N } (num\ of\ sensors) = \left({}^{P}/_{\beta}\right) \ln\left\{e\beta\left({}^{f_U}/_{f_L}\right)\right\} = \ 2P * \ln\{9e\beta\}$$

P: Aperture length

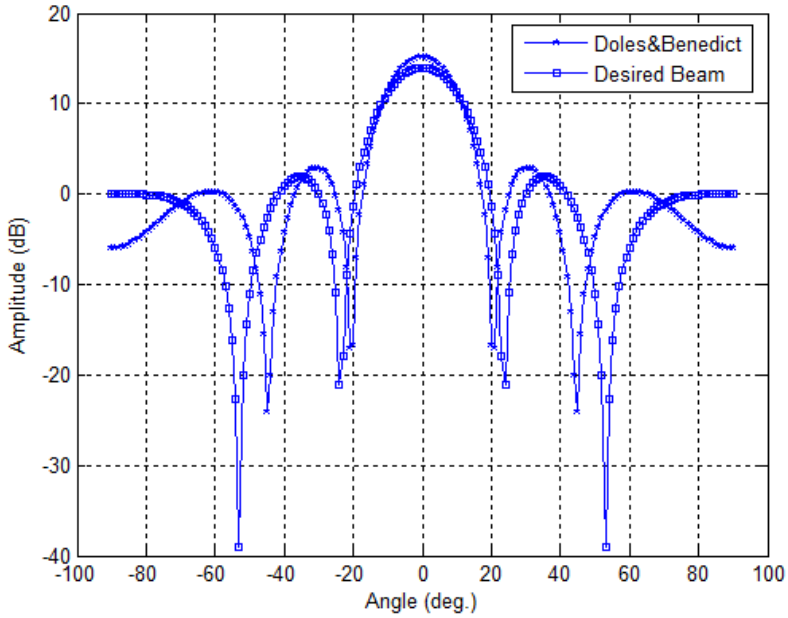

Figure 4.13: Comparison of the beam pattern obtained by Doles' & Benedict's method with desired pattern for aperture length P=5$*\frac{\lambda_L}{2}$ and N=15

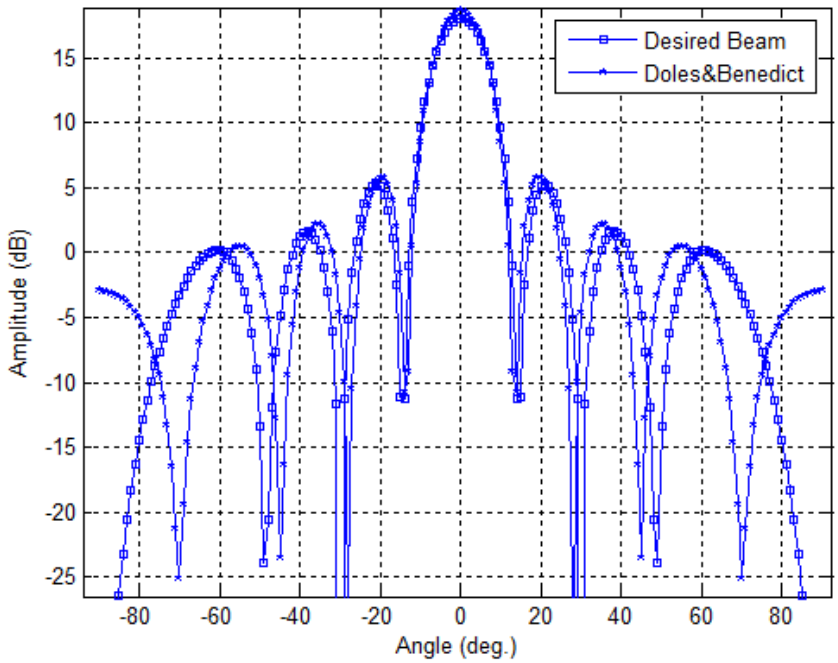

Figure 4.14: Comparison of the beam pattern obtained by Doles' & Benedict's method with desired pattern for aperture length P=8$*\frac{\lambda_L}{2}$ and N=25

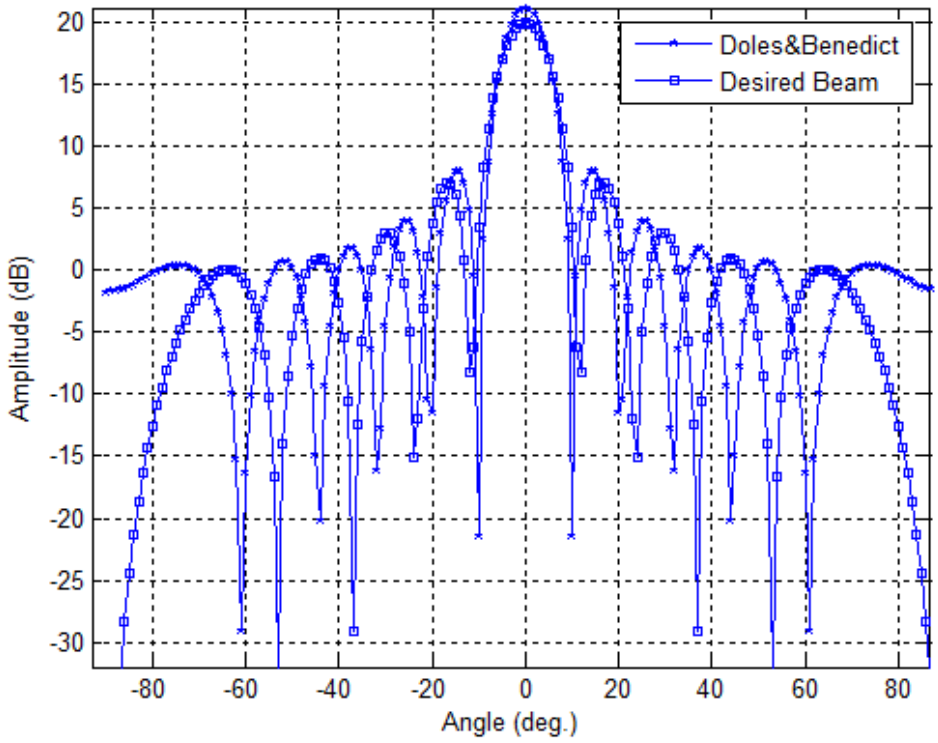

Figure 4.15: Comparison of the beam pattern obtained by Doles' & Benedict's method with desired pattern for aperture length P=10∗ $\frac{\lambda_L}{2}$ and N=31

As said above, increasing the aperture length increases the number of sensors used. Using more sensors gives a better estimate of the desired beampattern. But, as can be seen in the figures 4.13, 4.14, and 4.15, the method is not successful in estimating deep nulls.

Lastly, it is useful to remember that Doles' and Benedict's method doesn't have the capability of working with any desired beampattern, there is only one type of desired beampattern.

4.2.3 Ward's & Kennedy's Method

As done in 4.2.2, the performance of the method will be qualified with respect to two ciriteria:

4.2.3.1 How much the method is successful in obtaining a frequency invariant beampattern in any frequency band?

Constant parameters: $f_L = 2\ GHz$, $f_U = 18\ GHz$

N (Num. of sensors)= $P + 1 + \left\lceil \frac{\ln\left(\frac{f_U}{f_L}\right)}{\ln\left(\frac{P}{P-1}\right)} \right\rceil = P + 1 + \left\lceil \frac{\ln(9)}{\ln\left(\frac{P}{P-1}\right)} \right\rceil$.

P: Aperture length

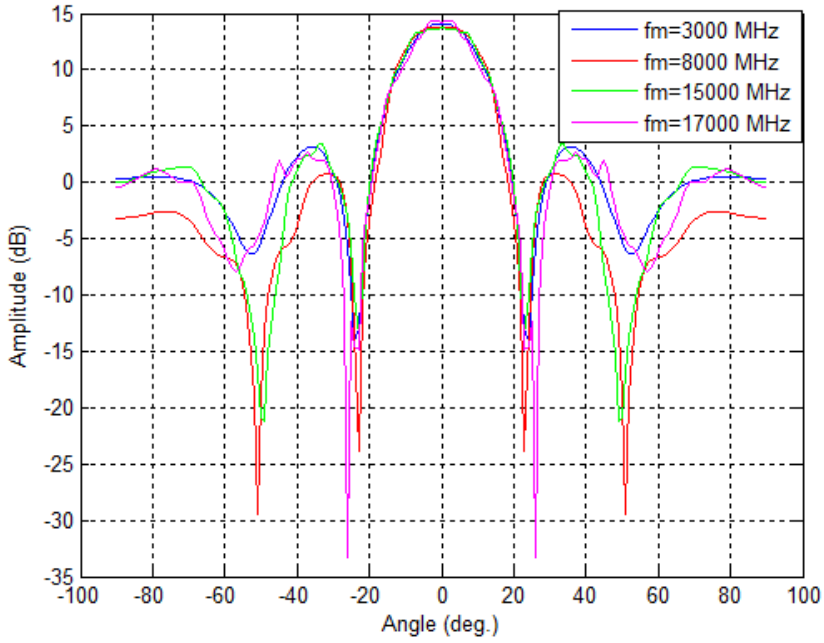

Figure 4.16: Obtained beam patterns for aperture length P=5* $\frac{\lambda_L}{2}$ and N=16

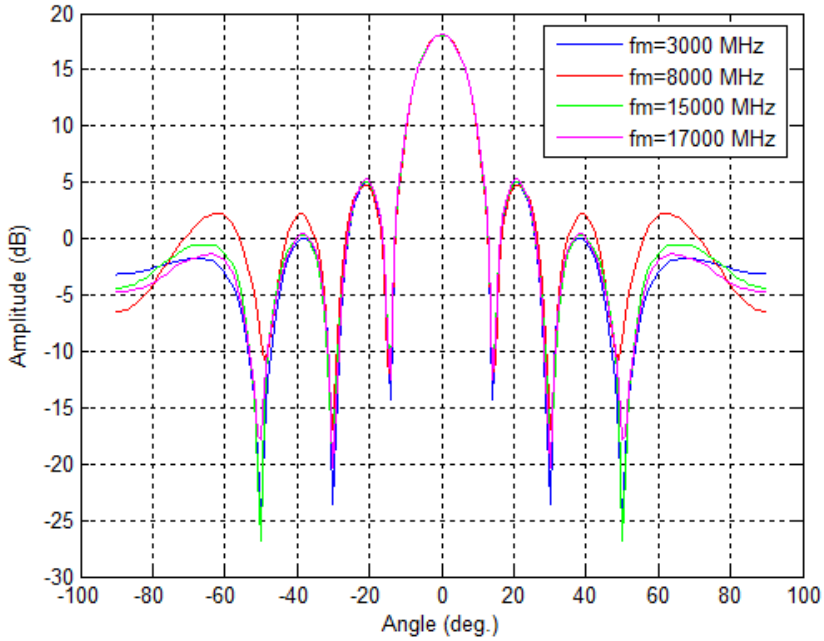

Figure 4.17: Obtained beam patterns for aperture length P=8* $\frac{\lambda_L}{2}$ and N=26

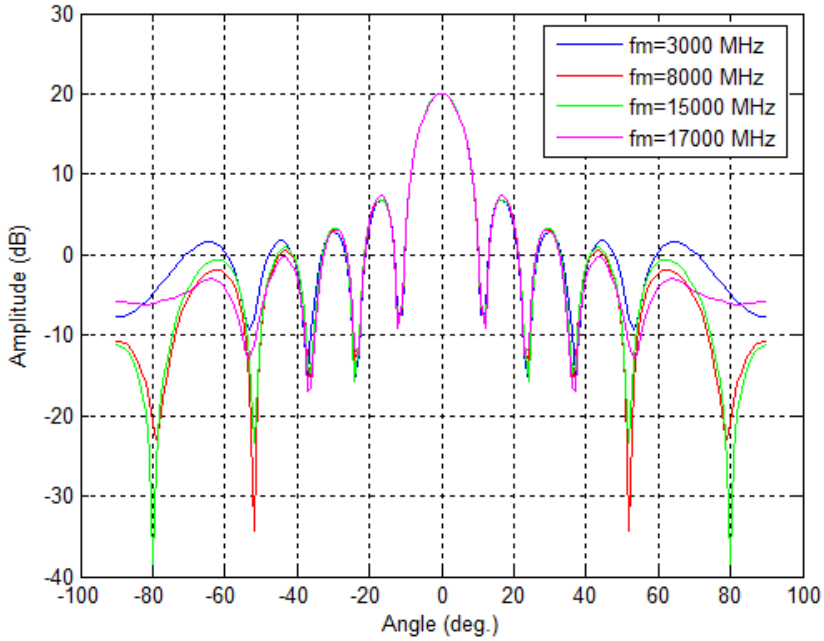

Figure 4.18: Obtained beam patterns for aperture length P=10* $\frac{\lambda_L}{2}$ and N=32

The succession in obtaining a frequency invariant beampattern increases when the aperture length increases, because of the same reason as that in Doles' & Benedict's method. This method and Doles' & Benedict's method performs similarly at this criterion.

4.2.3.2 How much the method is successful in obtaining desired beampattern at any operating frequency?

Constant parameters: $f_L = 2\ GHz$, $f_U = 18\ GHz$, $f_m = 8\ GHz$

N (Num. of sensors)= $P + 1 + \left\lceil \frac{\ln\left(\frac{f_U}{f_L}\right)}{\ln\left(\frac{P}{P-1}\right)} \right\rceil = P + 1 + \left\lceil \frac{\ln(9)}{\ln\left(\frac{P}{P-1}\right)} \right\rceil$.

P: Aperture length

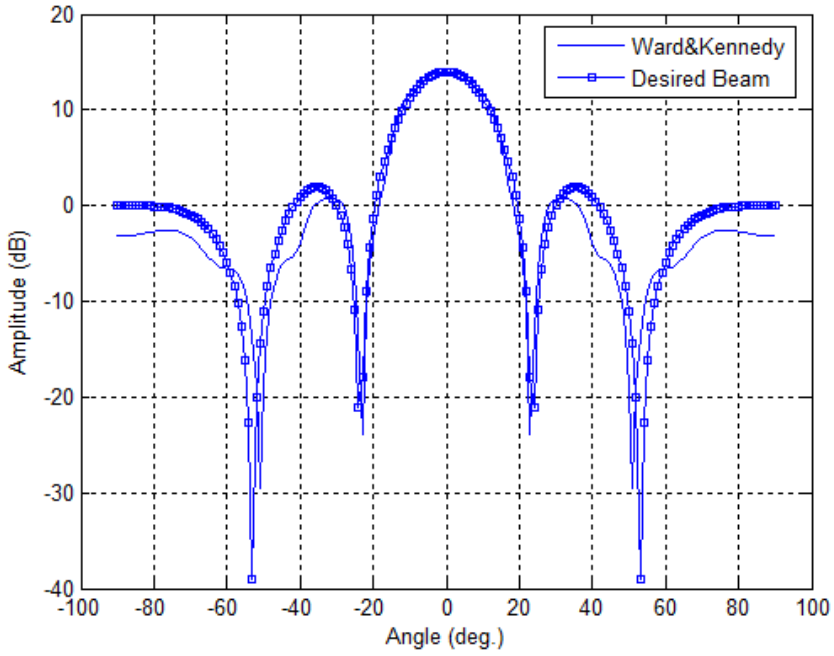

Figure 4.19: Comparison of the beam pattern obtained by Ward's & Kennedy's method with desired pattern for aperture length P=5* $\frac{\lambda_L}{2}$ and N=16

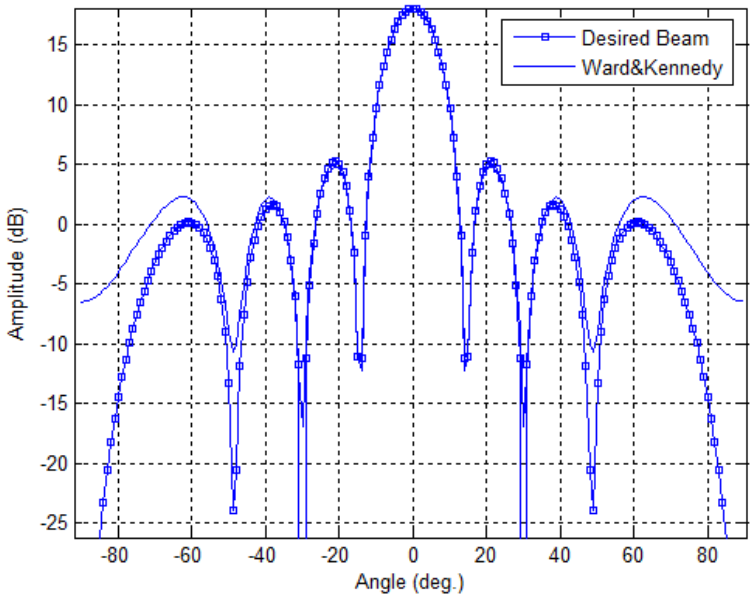

Figure 4.20: Comparison of the beam pattern obtained by Ward's & Kennedy's method with desired pattern for aperture length P=8* $\frac{\lambda_L}{2}$ and N=26

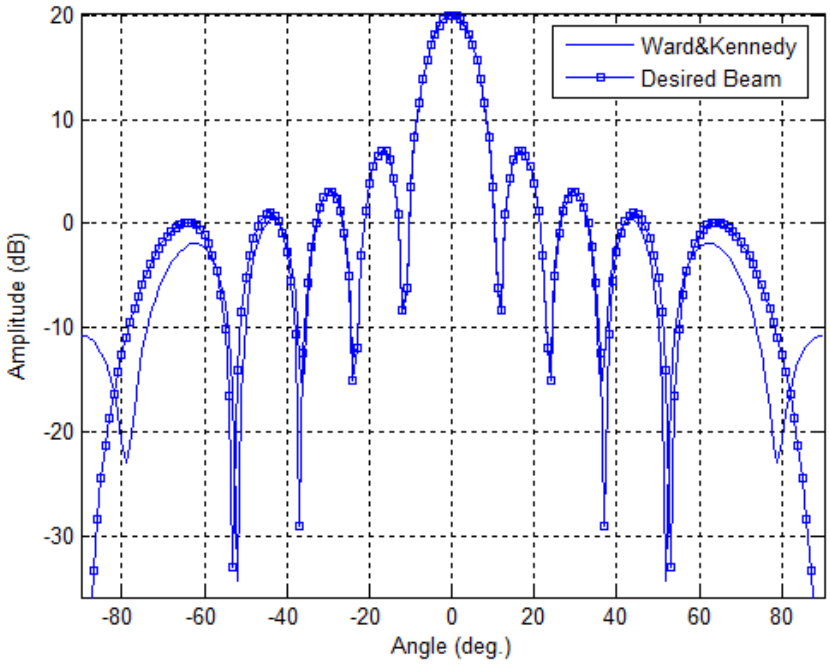

Figure 4.21: Comparison of the beam pattern obtained by Ward's & Kennedy's method with desired pattern for aperture length P=10* $\frac{\lambda_L}{2}$ and N=32

If we need to compare Ward's & Kennedy's method with Doles' & Benedict's method, we can say Ward's & Kennedy's method is more successful in obtaining the desired beam pattern. The deep nulls are estimated better than Doles' & Benedict's method. Also, note that Ward's & Kennedy's method can be used with any desired beam pattern.

CHAPTER 5

APPLICATION OF FREQUENCY INVARIANT BEAMFORMING TO WIDEBAND DOA ESTIMATION

In this chapter a wideband DOA estimation method based on Ward & Kennedy's FIB method is explained, and it is compared with the CSSM, the incoherent method and narrowband MUSIC.

The new wideband DOA method, we explain here, performs broadband focusing using time-domain processing rather than frequency decomposition. The proposed method removes the requirement to perform frequency decomposition.

5.1 Wideband DOA Estimation with FIB Method Using the Asymptotic Theory of Unequally Spaced Arrays

The method is told in [12]. It uses a beamspace preprocessing structure based on frequency-invariant beamforming. ***In this section we use square brackets to indicate time index where the data is collected and round brackets*** for the frequency responses.

As can be remembered from Chapter 3, the wideband methods like CSSM need to divide the frequency band into narrow bins before obtaining the composite covariance matrix. In this method, a set of beam shaping filters are used to focus the

received array data in the time domain so that there is no need for frequency decomposition.

The method consists of a filter and sum structure as shown in Figure 4.2. The sensor filters perform the role of beam shaping and ensure that the beam shape is constant as a function of frequency.

The output of the beamformer to a plane wave arriving from angle Θ is

$$r(\theta, f) = f \sum_{n=1}^{N} g_n H_n(f)\ e^{j2\pi f \tau_n(\theta)} \tag{5.1}$$

where $\tau_n(\theta)$ is the propagation delay to the *n*th sensor. (5. 1) can be rewritten as

$$r(\theta, f) = \boldsymbol{b}^H(f)\ \boldsymbol{a}(\theta, f) \tag{5.2}$$

where

$$\boldsymbol{b}(f) = f\ [g_1 H_1(f), \ldots, g_N H_N(f)]^H \tag{5.3}$$

$$\boldsymbol{a}(\theta, f) = \left[e^{j2\pi f \tau_1(\theta)}, \ldots, e^{j2\pi f \tau_N(\theta)}\right]^T \tag{5.4}$$

Through proper design as told in [12] and illustrated in Chapter 4 the output of the beamformer can be constant with respect to frequency variation over a design band, i.e.

$$r(\theta, f) = \boldsymbol{b}^H(f)\ \boldsymbol{a}(\theta, f) = r_{FI}(\theta) \qquad \forall\theta,\ \forall f \in [f_L,\ f_U] \tag{5.5}$$

5.1.1 For Linear Array

Consider a linear array of N sensors whose sensors are not necessarily uniformly spaced and D far-field broadband signals where D < N. The time series received by the *n*th sensor is,

$$y_n[k] = \sum_{d=1}^{D} s_d[k - \tau_n(\theta_d)] + v_n[k] \tag{5.6}$$

where $s_d[k]$ is the *d*th source signal, and $v_n[k]$ is additive white noise. The frequency response of the time series is

$$y_n(f) = \sum_{d=1}^{D} e^{j2\pi f \tau_n(\theta_d)} s_d(f) + v_n(f) \tag{5.7}$$

The vector of time series and the frequency response vector corresponding to that vector are given by

$$\boldsymbol{y}[k] = [y_1[k], \ldots, y_N[k]]^T \tag{5.8}$$

$$\boldsymbol{y}(f) = \boldsymbol{A}(\theta, f)\boldsymbol{s}(f) + \boldsymbol{v}(f) \tag{5.9}$$

where $\boldsymbol{A}(\theta, f) = [\boldsymbol{a}(\theta_1, f), \ldots, \boldsymbol{a}(\theta_D, f)]$ is the NxD source direction matrix. If FIB is applied to the output of the sensors, the beamformer output is

$$z[k] = \sum_{n=1}^{N} \sum_{m=0}^{M-1} b_n[m] y_n[k - m] \tag{5.10}$$

$$z(f) = \boldsymbol{b}^H(f)\boldsymbol{y}(f) \tag{5.11}$$

Let us assume that we form J different beamformers such that D < J ≤ N. Then the beamformer output vector is given by

$$\boldsymbol{z}(f) = [z_1(f), \ldots, z_J(f)]^T = \begin{bmatrix} \boldsymbol{b}_1^H(f) \\ \vdots \\ \boldsymbol{b}_J^H(f) \end{bmatrix} \boldsymbol{y}(f) \tag{5.12}$$

where $b_j(f)$ is the jth set of beamforming filter responses. The beamformer outputs should cover a spatial sector where the broadband sources lie and should have low sidelobe levels to attenuate unwanted sources and false target detections. Let $\boldsymbol{C}(f) = [\boldsymbol{b}_1(f), \ldots, \boldsymbol{b}_J(f)]$ be the NxJ beamforming matrix. If we use (5.9) in (5.12).

$$\begin{aligned} \boldsymbol{z}(f) &= \boldsymbol{C}^H(f)\boldsymbol{A}(\theta, f)\boldsymbol{s}(f) + \boldsymbol{C}^H(f)\boldsymbol{v}(f) \\ &= \boldsymbol{A}_c(\theta, f)\boldsymbol{s}(f) + \boldsymbol{v}_c(f) \end{aligned} \tag{5.13}$$

where $\boldsymbol{A}_c(\theta, f) = \boldsymbol{C}^H(f)\boldsymbol{A}(\theta, f)$ is the JxD FIBS source direction matrix. Since the beamformers make the overall beam pattern of the array approximately frequency invariant in the design band, the FIBS source direction matrix is approximately constant for all frequencies in the design band:

$$\boldsymbol{A}_c(\theta, f) \approx \boldsymbol{A}_c(\theta)\ ,\ \forall f \in [f_L, f_U] \tag{5.14}$$

As a result, we can obtain only one covariance matrix, i.e. the FIBS data covariance matrix, for all of the design band without dividing it into narrowbands:

$$\boldsymbol{R}_z(f) = E\{\boldsymbol{z}(f)\boldsymbol{z}^H(f)\} \implies \boldsymbol{R}_z = \int_{f_L}^{f_U} \boldsymbol{R}_z(f)df = \boldsymbol{A}_c(\theta)\boldsymbol{R}_s\boldsymbol{A}_c(\theta)^H + \boldsymbol{R}_v \quad (5.15)$$

After obtaining the FIBS data covariance matrix, we can apply any narrowband subspace method to estimate AOAs of the broadband sources.

5.2 Simulations

Before giving simulation results, we should determine a constant sampling rate to accurately sample all signals of interest. We will take the maximum bandwidth allowed for a wideband signal as the half of central frequency, i.e, bandwidth / $f_c \leq$ 0.5. The band of operation for which we design the nonuniform antenna placement given by 4.34 will be 2-18 MHz. Then, the maximum sampling rate of the receiver with respcet to Nyquist sampling rate is

Sampling:

Band of operation = 2 – 18 MHz

Maximum bandwidth allowed = f_c / 2 = 18 / 2 = 9 MHz

Sampling rate= 18 MHz

Also, the receiver should have a frequency estimation accuracy. Let's assume we require to estimate frequencies with 10 KHz error:

Frequency Estimation:

$\Delta f * \Delta T \geq 1/ 2\pi \rightarrow \Delta T \geq 1 / (2\pi * \Delta f) \approx 16$ usec.

Then we can take the minimum observation time equal to 20 usec. As a result the minimum snapshot number taken while minimum observation time is SN=360.

The test signal is a wideband signal generated as a sum of complex exponentials

$$s(t) = \sum_{n=0}^{N_f-1} \exp\left(j2\pi f_n t + \mu_n\right) \tag{5.16}$$

where μ_n is a uniformly distributed random variable over $[0, 2\pi)$.

The two overall beam patterns of a 7-element linear array formed by Ward & Kennedy's method can be seen in figure 5.1. The overall beampatterns are the outputs of the beamforming filters told in section 4.1.3 and 5.1. The overall beampatterns are separated by a definite angle called "squint angle" and can be seen in figure 5.1.

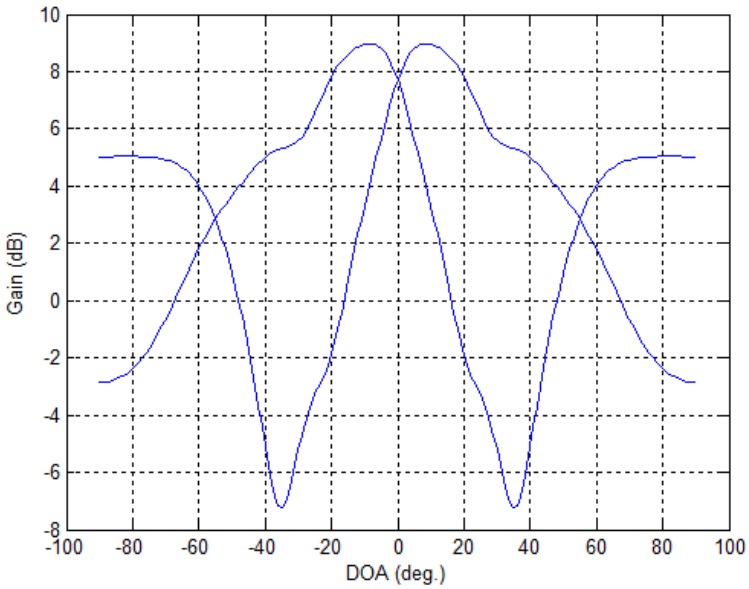

Figure 5.1: Overall beam patterns formed by Ward & Kennedy's method when aperture width is P=2 and squint angle=10°

In simulations, a 7-element linear array is used corresponding to $P=2*\lambda_L/2$ aperture width where λ_L is the wavelength of the lower frequency of band.

SNR Definition:

The wideband signal used in the simulations is generated by summing a set of complex exponentials that are narrowband signals having unity gain (5.16). SNR is defined in terms of one of these complex exponential signals, i.e, the power of one complex exponential is used as the signal power in SNR calculation. That is, for the received signal r(t) given below

$$r(t) = \sum_{n=0}^{N_f-1} A_n \exp(j2\pi f_n t + \mu_n) + w(t) \quad , \qquad \mu_n \in [-\pi, \pi] \tag{5.17}$$

f_n: $frequency\ of\ the\ n^{th}\ bin$

the SNR for the k^{th} bin is defined as $|A_k|^2/N_0$ where N_0 is the variance of the white noise process w(t). In this study, we take $A_k=1$ for all bins and vary N_0 to change the value of the operational SNR.

5.2.1 Performance Analysis of Wideband DOA Estimation with FIB Method Using the Asymptotic Theory of Unequally Spaced Arrays

We will investigate the effect of some factors to the performance of our wideband DOA estimation method. These factors are

- Signal to Noise Ratio (SNR)
- Central frequency of wideband signal
- Squint angle between overall beams
- Number of overall beams used in DOA estimation

- Snapshot Number
- Quality of the initial estimation of the DOA of target
- Quality of the estimation of central frequency

5.2.1.1 Signal to Noise Ratio

Constant parameters:

Number of overall beams=2, P=2*λ_L/2, DOA=30°, f_L=2 MHz, f_U=18 MHz Bandwidth= f_c / 5, f_c=10 MHz, Squint Angle= 35°, Observation Time=20 usec, Snapshot Number=50, Number of trials=10000

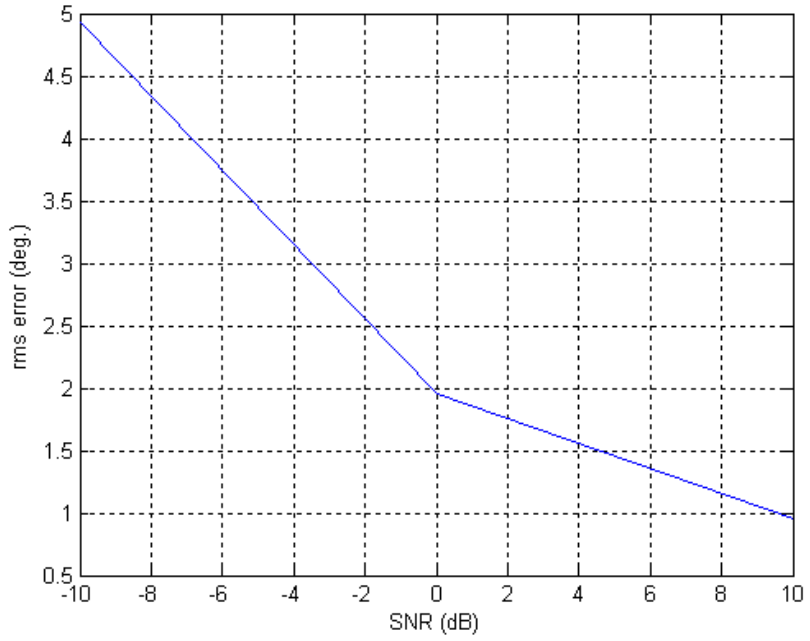

Figure 5.2: SNR versus rms error for Ward & Kennedy's FIB method

As can be seen in the figure above, FIB method is not very successful at low SNR. We can use Ward & Kennedy's FIB method with high accuracy at middle and high SNR.

5.2.1.2 Central Frequency of Wideband Signal

Constant parameters:

SNR= 0 dB, Number of overall beams=2, P= $2*\lambda_L / 2$, DOA=30°, f_L=2 MHz f_U=18 MHz, Bandwidth= $f_c / 5$, Squint Angle= 35°, Observation Time=20 usec, Snapshot Number=50, Number of trials=10000

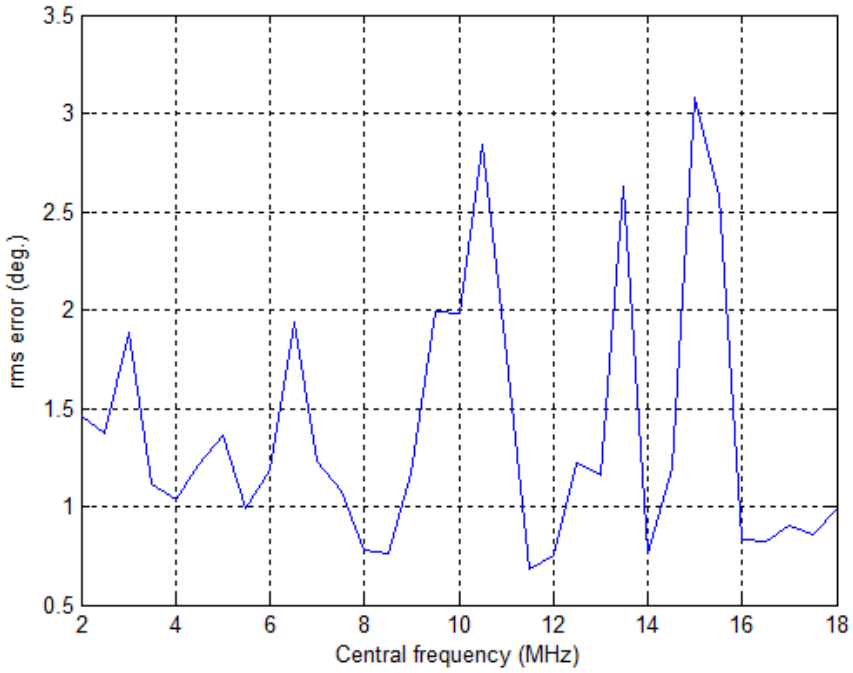

Figure 5.3: Central frequency versus rms error for Ward & Kennedy's FIB method

In figure 5.3, a uniform error pattern can't be seen. There can be three reasons for this: Primary filter design, antenna placement and iteration number. Iteration number was 10000 so that it doesn't seem reasonable that ripples occur because of iteration number. Also we will see in section 5.4 that antenna placement used in Ward & Kennedy's FIB method doesn't create ripples in error pattern.

5.2.1.3 Bandwidth of Wideband Signal

Constant parameters:

SNR= 0 dB, Number of overall beams=2, P= $2*\lambda_L$ / 2, DOA=30°, f_L=2 MHz f_U=18 MHz, f_c= 10 MHz, Squint Angle= 35°, Observation Time=20 usec, Snapshot Number=50, Number of trials=10000

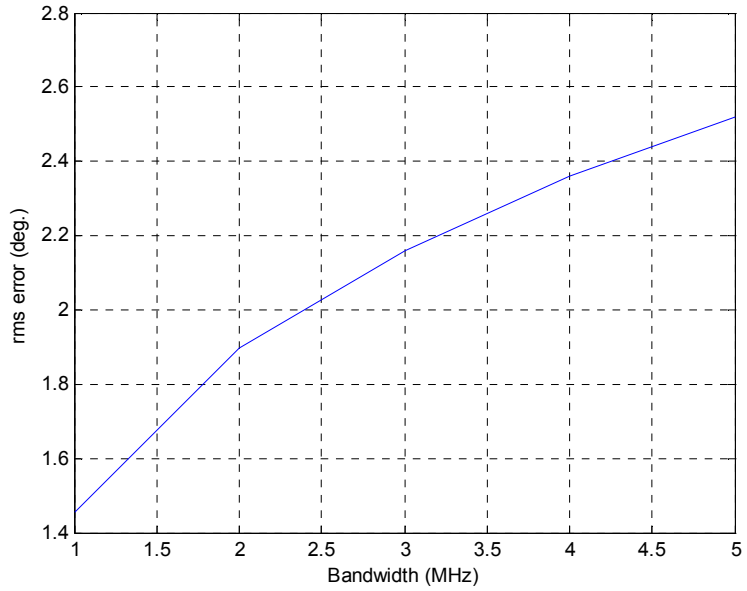

Figure 5.4: Bandwidth of signal versus rms error for Ward & Kennedy's FIB method

In ideal, bandwidth has no effect on DF performance. But we can't design primary filters as in ideal so that frequency invariancy of the overall beams used in DOA estimation loses its validity more as the bandwidth becomes larger.

5.2.1.4 Squint Angle Between Overall Beams

Constant parameters:

SNR= 0 dB, Number of overall beams=2, P= $2*\lambda_L$ / 2, DOA=30°, f_L=2 MHz, f_U=18 MHz, f_c= 10 MHz, Bandwidth= f_c / 5, Observation Time=20 usec, Snapshot Number=50, Number of trials=8000

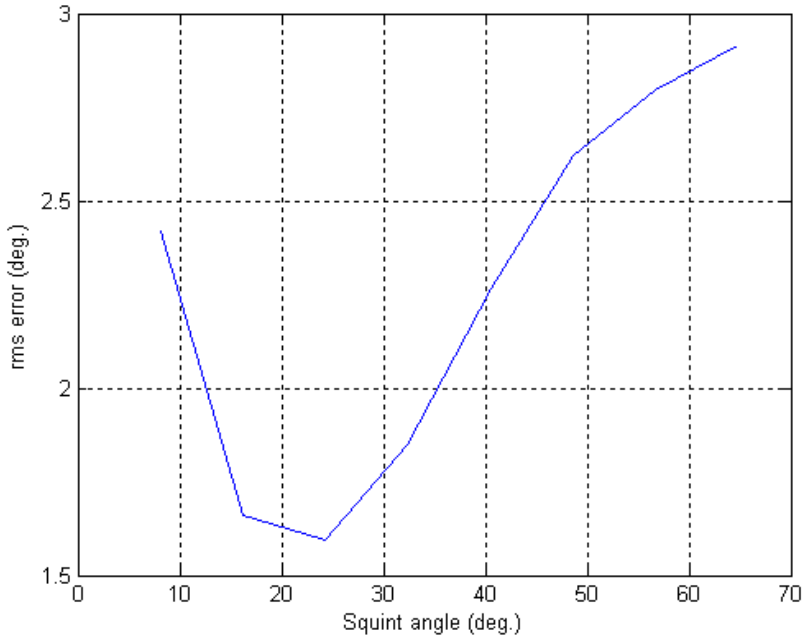

Figure 5.5: Squint Angle versus rms error for Ward & Kennedy's FIB method

When the squint angle is gradually increased from zero, an optimum value for the minimum rms estimation error is determined. In figure 5.6, this optimum value is between 20° and 30°. (An exact value can't be given because of the discrete squint angle set used in the simulation.) The beamwidth of the estimated beam pattern is nearly 60° so that the optimum value is around 30° for an exponential pattern. However, the beampattern used in the DOA estimation is an approximation which is obtained by properly summing 7 omni-directional antenna outputs, so we do not expect the optimum value to be exactly the same as the one of an exponential pattern.

5.2.1.5 Number of Overall Beams

a. Field of View Width is not Constant

Constant parameters:

SNR= 0 dB, P= $2*\lambda_L$ / 2, DOA=30°, f_L=2 MHz, f_U=18 MHz, f_c= 10 MHz Bandwidth= f_c / 5, Squint Angle= 35°, Observation Time=20 usec, Snapshot Number=50, Number of trials =8000

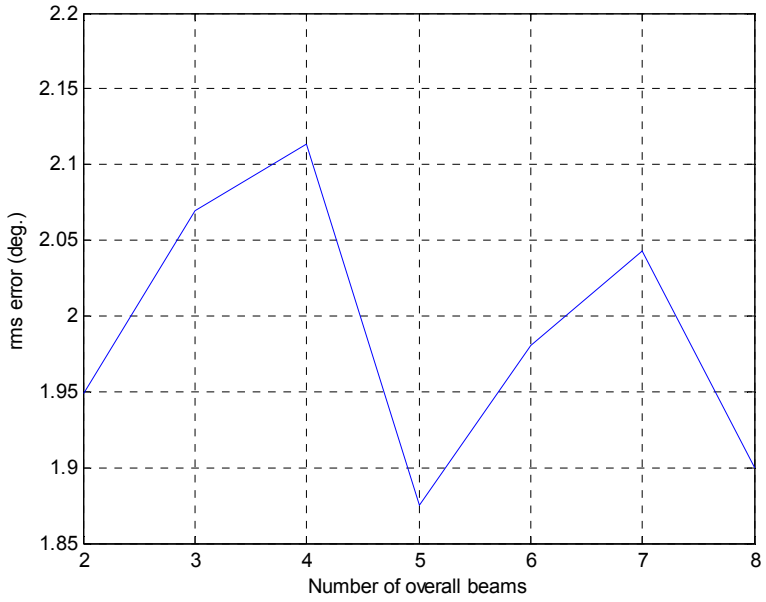

Figure 5.6: Number of overall beams versus rms error for Ward & Kennedy's FIB method

The width of FOV is important for quality initial estimation of the DOA of target, it should be wide enough to cover initial estimation region. When we take the standard deviation of initial estimation as being 10°, number of overall beams has no effect as can be seen in figure 5.6.

b. Field of View Width is Constant

Constant parameters:

SNR= 0 dB, P= $2*\lambda_L$ / 2, DOA=30°, f_L=2 MHz, f_U=18 MHz, f_c= 10 MHz Bandwidth= f_c / 5, Observation Time=20 usec, Snapshot Number=50, Number of trials=10000, Squint Angle= 90° / NumberOfOverallBeams

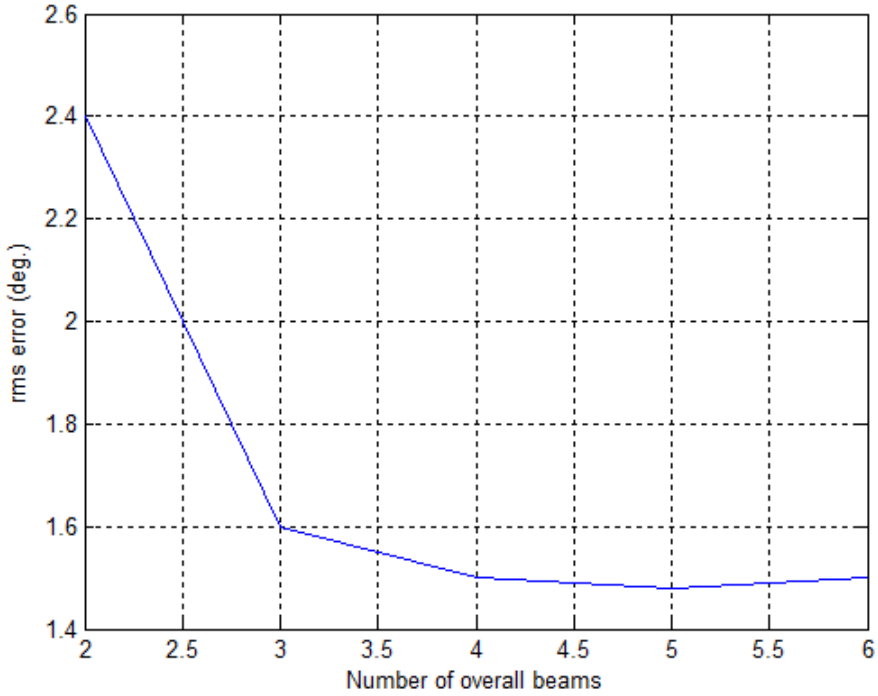

Figure 5.7: Number of overall beams versus rms error for Ward & Kennedy's FIB method

The performance of the FIB method is dependent on both squint angle and number of overall beams. If we hold the FOV constant and increase the number of overall beams, the performance will improve much at the beggining, but the improvement will slow down when increasing the number of overall beams more. Because we decrease the squint angle below the optimal value and change the steering angles of the beams if we increase number of overall beams more and more.

5.2.1.6 Snapshot Number

Constant parameters:

SNR= 0 dB, Number of overall beams=2, P= $2*\lambda_L$ / 2, DOA=30°, f_L=2 MHz f_U=18 MHz, f_c= 10 MHz, Bandwidth= f_c / 5, Squint Angle= 35°, Observation Time=20 usec, Number of trials=10000

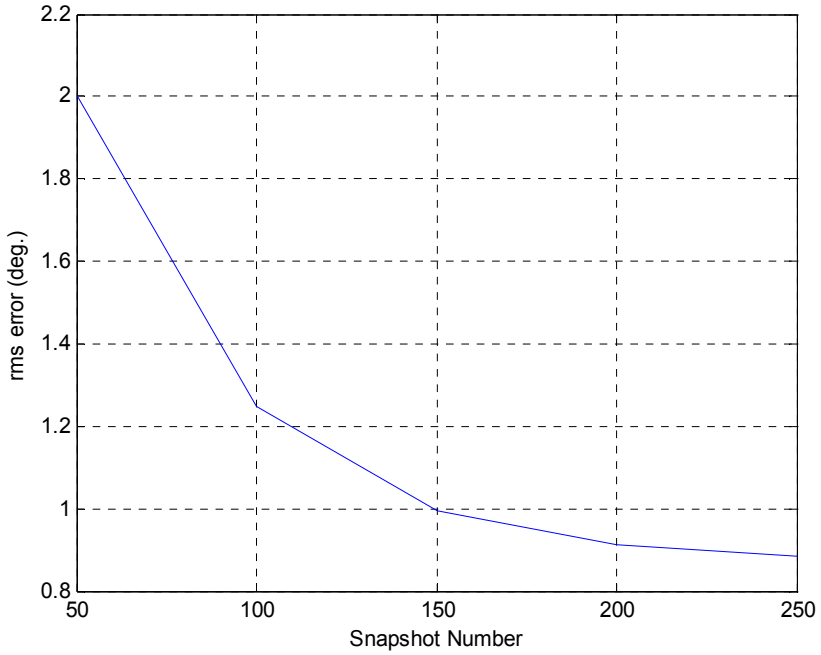

Figure 5.8: Snapshot Number versus rms error for Ward & Kennedy's FIB method

Naturally, increasing the snapshot number improves DF performance.

5.2.1.7 Quality of the Initial Estimation of DOA

Constant parameters:

SNR= 0 dB, Number of overall beams=2, P= $2*\lambda_L$ / 2, DOA=30°, f_L=2 MHz f_U=18 MHz, f_c= 10 MHz, Bandwidth= f_c / 5, Squint Angle= 35°, Observation Time=20 usec, Snapshot Number =50, Number of trials=10000

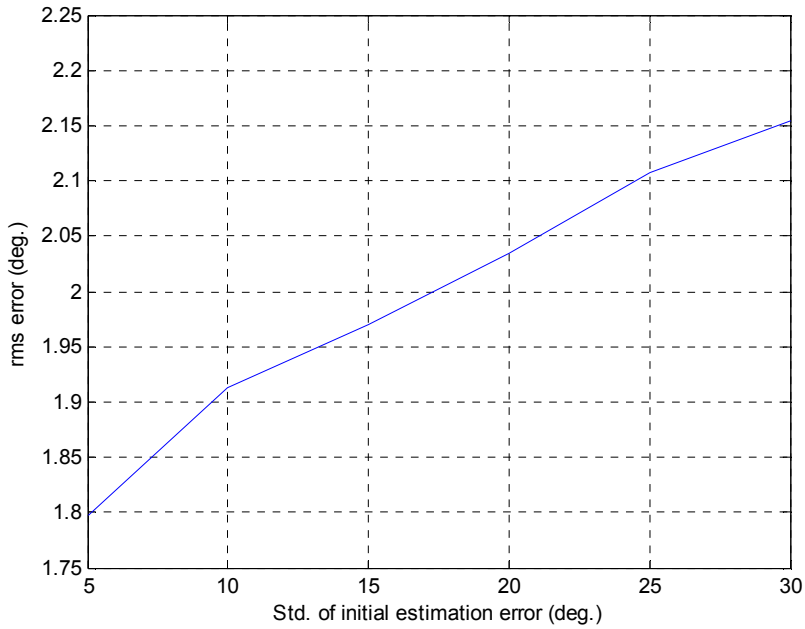

Figure 5.9: Std. of initial estimation error versus rms error for Ward & Kennedy's FIB method

Since the width of FOV when overall beam number is two is enough to cover initial estimation region, there is little effect of initial estimation on DF performance. The reason of little change in performance can be probability distribution characteristic of initial estimation error, we assume that it is uniform so that initial estimation error can take very high values.

5.2.1.8 Quality of the Estimation of Central Frequency

SNR= 0 dB, Number of overall beams=2, P= $2*\lambda_L$ / 2, DOA=30°, f_L=2 MHz f_U=18 MHz, Bandwidth= f_c / 5, Squint Angle= 35°, Observation Time=20 usec, Snapshot Number=50, Number of trials=10000

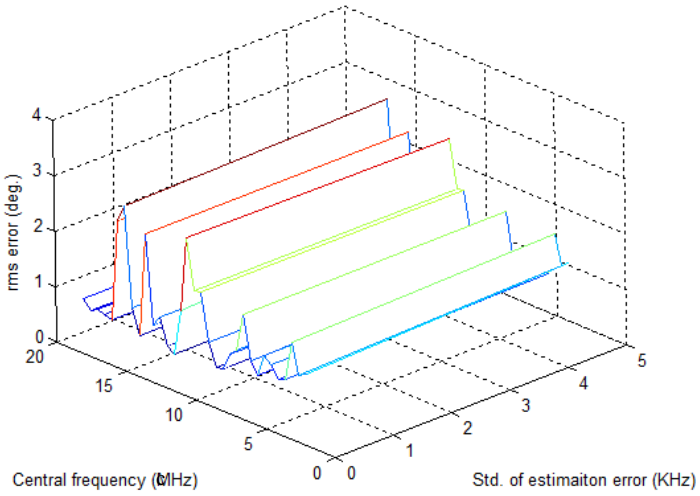

Figure 5.10: Noise Std. of central frequency estimation versus rms error for Ward & Kennedy's FIB method

In practice, frequency estimator in a receiver can make nearly 5 KHz rms error in 2-18 MHz frequency band when SNR= 0 dB. As can be seen in fig. 5.10, there is little effect of error made in central frequency estimation, at least, up to 5 KHz standard deviation.

5.2.2 Comparison of CSSM and Ward & Kennedy's FIB method

Shared Parameters :

Number of Antennas=7, Aperture width(P)=$2*\lambda_L/2$ (f_L=2 MHz), Bandwidth=$f_c/5$ Number of trials=5000, DOA=30° , f_c=6 MHz, Observation Time=20 usec, Snapshot Number=50

CSSM parameters:

Number of frequency bins= 32, d= P / (N-1) ($\lambda/2$ at f_c=6 MHz), Reference Frequency= c / (2*d)

FIB parameters:

f_L=2MHz, f_U=18MHz, Number Of Overall Beams=3, Squint angle=23°

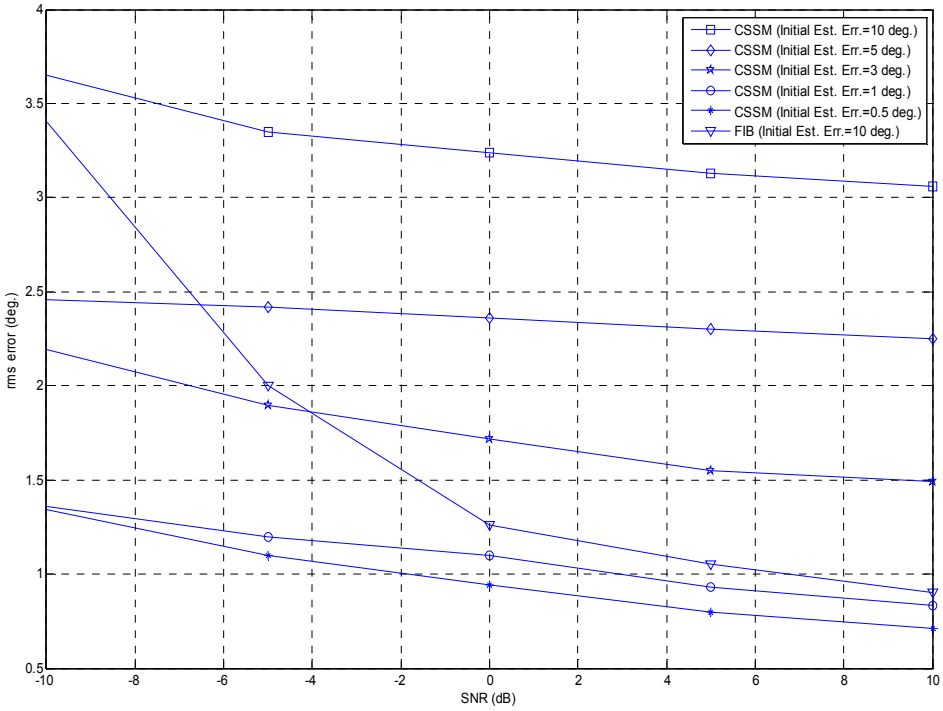

Figure 5.11: SNR versus rms error for CSSM and Ward & Kennedy's FIB method

As you can see in the figure, CSSM doesn't show a good performance at high initial estimation error. However, when decreasing the inital estimation error, CSSM' s performance improves and becomes better than that of the FIB method. As seen in Figure 5.9, the initial estimation error doesn't effect the FIB method's performance significantly. As a result, the FIB method can be a better solution at high initial estimation errors while CSSM works better at low initial estimation error.

5.2.3 Comparison of Incoherent Wideband Method and Ward & Kennedy's FIB Method

We compare incoherent wideband method and the FIB method. We use MUSIC algorithm at each narrowband bin and average the DOA estimates to get the incoherent wideband estimate. In this simulation, the central frequency of the

incoming signal matches the wavelength number of the uniform linear array used by MUSIC aglorithm (f_c=6 MHz). Therefore, we expect the best performance of narrowband MUSIC.

Shared Parameters :

Number of Antennas=7, Aperture width (P)=2*λ_L/2 (f_L=2 MHz), Bandwidth=f_c/5 Number of trials=5000, Snapshot Number= 50, DOA=30°, f_c=6 MHz, Observation Time=20 usec

Incoherent wideband method parameters:

d= P / (N-1) (λ/2 at f_c=6 MHz)

FIB parameters:

f_L=2MHz, f_U=18MHz, Number Of Overall Beams=3, Squint angle=23°

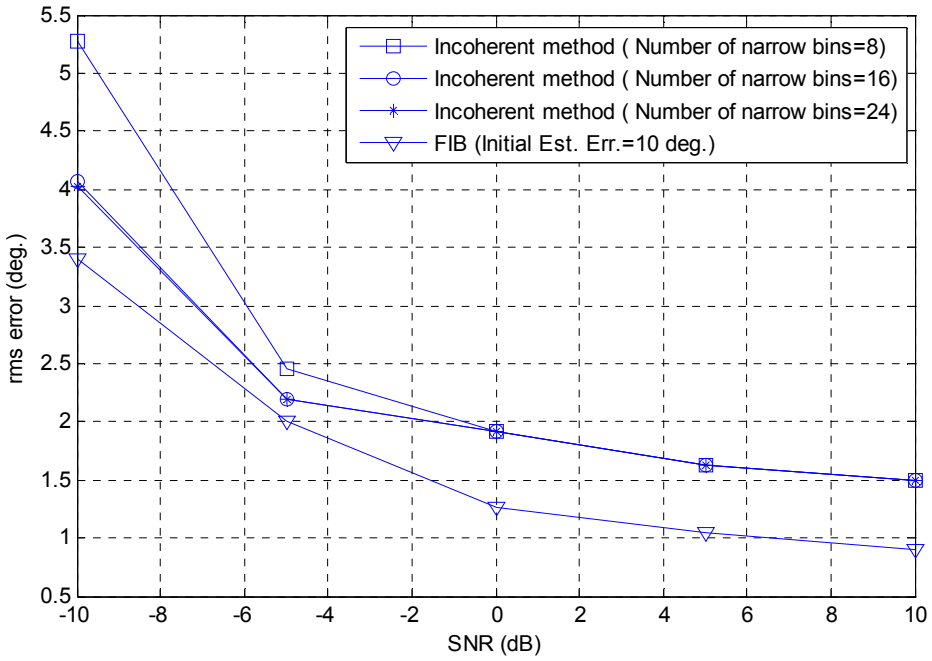

Figure 5.12: SNR versus rms error for Incoherent Wideband Method and Ward & Kennedy's FIB method

The FIB method is better at all SNR values than the incoherent wideband method in figure 5.12. However, it should be emphasized that the performance of the incoherent method is strictly dependent on the spectrum resolution, it shows a better performance when the resolution increases. If the band of the signal is decomposed into more frequency bins, there is no effect of this process to the performance. Because, the bins are processed independently from each other and we can't obtain a process gain as in CSSM. However, there is some improvement in performance at SNR=-10 dB, because the noise power is ten times bigger than signal power and processing a more narrow bin decreases the effect of noise.

5.2.4 Comparison of Narrowband MUSIC and Ward & Kennedy's FIB Method

It should be emphasized that a single frequency bin obtained by decomposing the band of the signal is used to estimate DOA by narrowband MUSIC.

Shared Parameters:

Number of Antennas=7, Aperture width(P)=$2*\lambda_L/2$, f_L=2 MHz, f_U=18 MHz, Bandwidth=$f_c/5$, Number of trials =5000, DOA=30°, f_c=6 MHz, Observation Time=20 usec, Snapshot Number=50

Narrowband MUSIC parameters:

Number of narrow bins= 8, 24

FIB parameters:

Number Of Overall Beams=3, Squint angle=23°

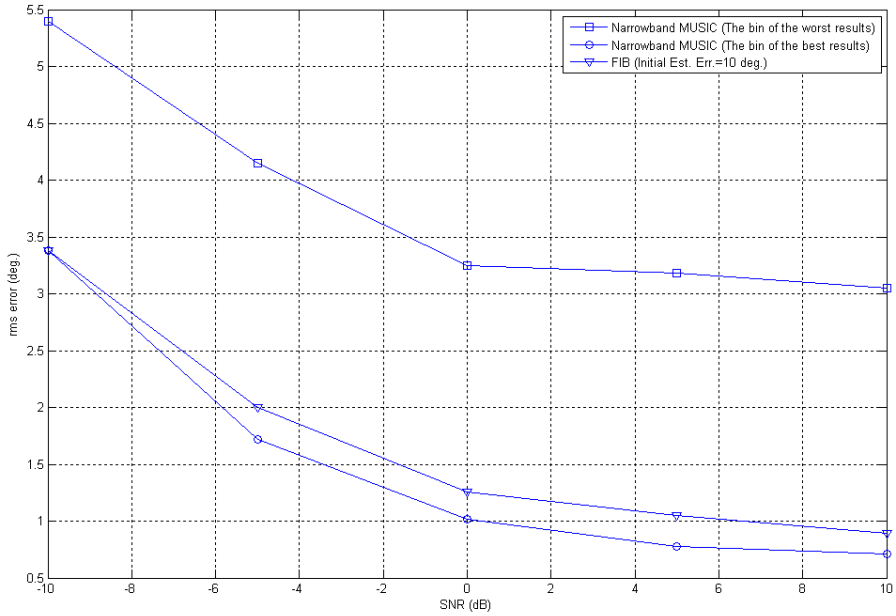

Figure 5.13: SNR versus rms error for Narrowband MUSIC (Number of overall beams=24) and Ward & Kennedy's method FIB method

The performance of narrowband MUSIC is strictly depedent on the narrow frequency bin used, and this result is obvious in figure 5.13. The best result obtained from narrow frequency bins can be better than that of the FIB method. But we need to decompose the band of the signal into narrow bins and process each separately. Also the channel number used must be equal to the number of sensors while we can use less channels for the FIB method.

CHAPTER 6

CONCLUSION

In this thesis, a special wideband DOA estimation method based on Ward & Kennedy's FIB method is examined. Then it is compared with simple Coherent Signal Subspace Method (CSSM), incoherent wideband method and narrowband MUSIC.

For Ward&Kennedy's FIB method, a linear array with the aperture width $2*(\lambda_L /2)$ is used where λ_L is the wavelength at f_L=2 MHz. Therefore, we obtain the minimum aperture width to implement the FIB algorithm, i.e., a 7-element non-uniform linear array is formed.

When Ward&Kennedy's FIB method is evaluated at different SNR values, we find out that the method doesn't have a good performance at low SNR values. Also, it doesn't show a constant DOA estimation performance at different central frequencies although it should be ideally invariant to all frequencies in the band of interest. The reason of this shortcoming can be the design of primary filters.

The number of overall beams is an important parameter for the FIB method. We need to design different filter banks for each overall beam, and they should be coherently phased. However, in practice establishing the phase coherency is a difficult problem so that using fewer number of overall beams is desired. As seen in Figure 5.7, the performance doesn't change much when more than three beams are implemented. Because we decrease the squint angle under the optimum squint angle if we increase number of overall beams much. Also we change the steering angles

of the overall beams whenever we change the number of overall beams, and this effects the performance too.

Other parameters such as snapshot number, initial estimate of DOA, etc. are also investigated and the results can be found in section 5.2.1.

Ward & Kennedy's FIB method is compared with CSSM in section 5.2.2. CSSM shows a bad performance when initial estimation error is high, because focusing matrix design quality is strongly dependent on the initial estimation error. On the other hand, the FIB method can compensate the initial estimation error better and its performance doesn't change much with this error. As a result, we can say that the FIB method can be preferred at high initial estimation error while CSSM is better at low error. (**Figure 5.11)** However, it must be emphasized that the FIB method is compared with CSSM method given in [3]. There are other coherent methods such as WAVES, [5] and there are also advanced versions of Coherent Signal Subspace (CSS) processing such as CSS using Rotational Signal-Subspace Matrix [16], robust CSS [17].

Although the FIB method is not better than CSSM at low initial estimation error, it has an important advantage. It doesn't need the same number of RF channels with the number of sensors. With the design of analog primary filters, we can decrease the number of receiver channels so the calibration of channels becomes easier to be achieved and the cost decreases.

In section 5.2.3, incoherent wideband method and the FIB method are compared. As expected, the incoherent method shows a bad performance at low SNR. It can be considered to be successful at high SNR. The FIB method processes all of the wideband signal at once while the incoherent method decomposes the band of the signal and processes each narrow bin independently from others so the FIB method is better in figure 5.12. However, it should be emphasized that the performance of the incoherent method is strictly dependent on the spectrum resolution, it shows a better performance when the resolution increases.

In section 5.2.4, narrowband MUSIC is compared with the FIB method. Narrowband MUSIC decomposes the band of the signal like the incoherent MUSIC, but uses the result of only one bin. The best one among the results obtained from narrow bins can be better than the result of the FIB method. However, narrowband MUSIC still needs as many channels as sensors.

As a result, the FIB method can be a good choice with its lower implementation cost when the initial estimation error is high. This result is critical for many practical systems.

REFERENCES

[1] Petre Stoica & Randolph L. Moses, “Introduction to Spatial Analysis”

[2] Sathish Chandran (Editor), “Advances In Direction-Of-Arrival Estimation”

[3] Wang, H., and M. Kaveh, “Coherent Signal-Subspace Processing for the Detection and Estimation of Angles of Arrival of Multiple Wide-Band Sources,”IEEE Trans. On Acoustics Speech, and Signal Processing,Vol. ASSP-33, August 1985, pp 823-831.

[4] Ta-Sung Lee, “Efficient Wideband Source Localization Using Beamforming Invariance Technique”, IEEE Transactions on SIGNAL PROCESSING, Vol. 42, No.6, June 1994

[5] Di Claudio, E.D., and R. Parisi, “WAVES: Weighted Average of Signal Subspaces for Robust Wideband Direction Finding”, IEEE Transactions on SIGNAL PROCESSING, Vol. 49, No.10, October 2001, pp. 2179-2190

[6] Viberg M., B. Ottersten, and T. Kailath, “Detection and Estimation in Sensor Arrays Using Weighted Subspace Fitting”, IEEE Transactions on SIGNAL PROCESSING, Vol. 39, November 1991, pp. 2436-2449

[7] Benjamin Friedlander, Fellow, IEEE, and Anthony J. Weiss, Senior Member, IEEE, “Direction Finding for wideband Signals Using an Interpolated Array”, IEEE Transactions on SIGNAL PROCESSING, Vol. 41, No.4, April 1993

[8] T. Chou, “Frequency Independent Beamformer with Low-Response Error”, Proc. ICASSP, Detroit, Michigan, vol. 5, pp. 2995-2998, 1995

[9] J. H. Doles, F. D. Benedict, “Broadband Array Design Using The Asymptotic Theory of Unequally Spaced Arrays”, IEEE Trans. Antennas Propagation, Vol. AP-36, pp 27- 33, January 1988

[10] Darren B. Ward, Rodney A. Kennedy, Robert C. Williamson, “Theory and Design of Broadband Sensor Arrays with Frequency Invariant Far-Field Beam Patterns”, J. Acoust. Soc. Am. 97, February 1995

[11] Darren B. Ward, Rodney A. Kennedy, and Robert C. Williamson, “FIR Filter Design for Frequency Invariant Beamformers”

[12] Darren B. Ward, Zhi Ding, and Rodney A. Kennedy, “Broadband DOA Estimation Using Frequency Invariant Beamforming”, IEEE Transactions On Signal Processing, Vol. 46, No.5, May 1998

[13] S. Sivanand, M. Kaveh, “Direct Design of Focusing Filters for Wideband Direction Finding”

[14] Wei Liu, Stephan Weiss, “Design of Frequency Invariant Beamformer for Broadband Arrays”

[15] H. L. Van Trees, “Optimum Array Processing, Part IV of Detection, Estimation, and Modulation Theory”, John Wiley & Sons, Inc., New York, U.S.A., 2002

[16] H. Hung & M. Kaveh , “A New Class Of Focusing Matrices For Coherent Signal-Subspace Method”, IEEE, 1988

[17] H. Hung & C. Mao, “Robust Coherent Signal-Subspace Processing for Directions-of-Arrival Estimation of Wideband Sources”, IEE Proc. Radar Sonar Navig., Vol. 141, No.5, October 1994

APPENDIX A

SHADING CONDITIONS AND DERIVATION OF BROADBAND ARRAY DESING CRITERIA FOR DOLES & BENEDICT'S METHOD

The aperture shading conditions are

$$W(v;\lambda) = 0, \quad v > S^{-1}(\beta\lambda/2)$$

$$W(v;\lambda) > 0, \quad v \le S^{-1}(\beta\lambda/2) \tag{A.1}$$

$$W(v;\lambda) > 0, \quad v > X^{-1}(P\lambda/2)$$

$$W(v;\lambda) > 0, \quad v \le X^{-1}(P\lambda/2) \tag{A.2}$$

and the amplitude shading conditions

$$W(v;\lambda)^2 = EX''(v)/X'(v), \quad \lambda/2 \le S(v) \le \beta\lambda/2, \quad \lambda_U \le \lambda \le \lambda_L \tag{A.3}$$

$$W(v;\lambda) = S(v)T(\lambda), \quad 0 \le v \le X^{-1}(P\lambda/2) \tag{A.4}$$

β and P parameters are

$$\beta = 2s_N\lambda_L^{-1} \tag{A.5}$$

$$P = 2L\lambda_L^{-1} \tag{A.6}$$

Where s_N is the largest spacing, $\lambda_L = c/f_L$ and $L=X(N)$ is the total length of the array.

If the first aperture shading condition is compatible with the second aperture shading condition, it is necessary that

$$S^{-1}(\beta\lambda/2) = X^{-1}(P\lambda/2) \tag{A.7}$$

At least for $\lambda_U \le \lambda \le \lambda_L$. The solution to (A.7) is

$$X(v) = Lr^{v-N} \tag{A.8}$$

Where

$$r = \exp(\beta/P) \tag{A.9}$$

Is the tapering parameter of the array. (A.8) must be valid at least for $P\lambda_u/2 \le X(v) \le P\lambda_L/2 = L$.

If sensor coordinates are given by (A.8), the first amplitude shading condition becomes

$$W(v;\lambda)^2 = E\beta / P, \qquad \lambda/2 \le S(v) \le \beta\lambda/2, \quad \lambda_u \le \lambda \le \lambda_L \tag{A.10}$$

Where E is called the sidelobe plateau level. For convenience the sidelobe plateau level is chosen to be $E = P/\beta$ so that $W(v;\lambda) = 1$ in that portion of the aperture.

If (A.7) is used with the second amplitude shading condition, we obtain

$$W(v;\lambda) = S(v)T(\lambda), \qquad 0 \le v \le S^{-1}(\beta\lambda/2) \tag{A.11}$$

Since $W(v;\lambda) = 1$ over the range $\lambda/2 \le S(v) \le \beta\lambda/2$, (A.11) is valid over the subrange $0 \le v \le S^{-1}(\lambda/2)$. $T(\lambda)$ is chosen to be $2/\lambda$ and (A.11) becomes

$$W(v;\lambda) = S(v)/(\lambda/2), \qquad 0 \le v \le S^{-1}(\lambda/2) \tag{A.12}$$